

**CZECH TECHNICAL UNIVERSITY IN PRAGUE**

**Faculty of Electrical Engineering**

**Department of Physics**



Bachelor Thesis:

**QCM analysis of nanoparticles and molecules**

Project of:                      Chen Xie

Supervisor:                     Bohuslav Rezek

Study program:   Electrical Engineering and Computer Science

Prague 2024



# BACHELOR'S THESIS ASSIGNMENT

## I. Personal and study details

Student's name:	<b>Xie Chen</b>	Personal ID number:	<b>485700</b>
Faculty / Institute:	<b>Faculty of Electrical Engineering</b>		
Department / Institute:	<b>Department of Electrical Power Engineering</b>		
Study program:	<b>Electrical Engineering and Computer Science</b>		

## II. Bachelor's thesis details

Bachelor's thesis title in English:

**QCM analysis of nanoparticles and molecules**

Bachelor's thesis title in Czech:

**QCM analýza nanočástic a molekul**

Guidelines:

Nanomaterials and especially nanoparticles can have a variety of functions from drug carriers to luminescent markers in biomedicine as well as components in electronic, energy harvesting and storage devices. The instructions for this work:

1. Get familiar with the recommended QCM literature.
2. Prepare your own overview of the current state of the art on the thesis topic.
3. Get familiar with the QCM device, software, and use for measurements.
4. Prepare sets of solutions of nanoparticles and molecules of various concentrations and compositions.
5. Analyze the samples by the QCM method. If feasible, complement by microscopic and spectroscopic characterizations.
6. Evaluate, present and discuss the obtained results in the thesis.

Bibliography / sources:

<https://www.sciencedirect.com/science/article/abs/pii/S0169433222005840> ; <https://pubs.acs.org/doi/10.1021/ac400468m>  
<https://www.sciencedirect.com/science/article/pii/S0925400522013910> ; <https://openqcm.com/>  
<https://pubs.rsc.org/en/content/articlelanding/2015/NR/C5NR00250H> ; <https://www.biolinscientific.com/faq/the-qcm-d-principle>

Name and workplace of bachelor's thesis supervisor:

**prof. RNDr. Bohuslav Rezek, Ph.D. Department of Physics FEE**

Name and workplace of second bachelor's thesis supervisor or consultant:

\_\_\_\_\_

Date of bachelor's thesis assignment: **21.09.2023** Deadline for bachelor thesis submission: \_\_\_\_\_

Assignment valid until: **16.02.2025**

\_\_\_\_\_  
prof. RNDr. Bohuslav Rezek, Ph.D.  
Supervisor's signature

\_\_\_\_\_  
doc. Ing. Zdeněk Müller, Ph.D.  
Head of department's signature

\_\_\_\_\_  
prof. Mgr. Petr Páta, Ph.D.  
Dean's signature

## III. Assignment receipt

The student acknowledges that the bachelor's thesis is an individual work. The student must produce her thesis without the assistance of others, with the exception of provided consultations. Within the bachelor's thesis, the author must state the names of consultants and include a list of references.

\_\_\_\_\_ Date of assignment receipt

\_\_\_\_\_ Student's signature

## **Declaration:**

“I hereby declare that this bachelor’s thesis is the product of my own independent work and that I have clearly stated all information sources used in the thesis according to Methodological Instruction No. 1/2009 – “On maintaining ethical principles when working on a university final project, CTU in Prague”

Date

.....

Author’s signature

.....

## **Acknowledgment:**

I would like to express my deepest gratitude to my supervisor, Bohuslav Rezek, for helping me find a topic that I enjoy and am interested in, as well as for taking time out of his busy schedule to be patient with me and assist me in successfully completing my project and thesis.

I would also like to thank Chakavak Esmaili for her generous help and advice on my experiments and thesis, as well as for her guidance when I was stressed out.

I am deeply grateful to Markéta Bařinková for her expertise in managing the Scanning Electron Microscope and procuring the SEM images vital for my research.

And finally, I would like to thank my parents for supporting me and giving me the confidence to overcome all the difficulties!

# Abstract

Sensors based on quartz crystal microbalances (QCM) have dominated research in recent years. They have produced excellent laboratory results in analyzing the mass as well as the conformation of nanoparticles and molecules. The technology is constantly developed and widely used in various fields of chemistry, physics and biology. Here, we investigated a novel concept based on the use of nanodiamonds on QCM and explored the performance of nanodiamonds on QCM sensors, which helps in expanding the application of nanodiamonds in biosensing and exploring their effectiveness in QCM setups. We established a procedure and suitable parameters for the QCM sensor measurement. 5 MHz open-source QCM sensor system was used for building up the sensor assay for detection of cortisol via antigen (Ag)-antibody (Ab) reactions. Optical pictures after each functionalization step as well as scanning electron microscopy (SEM) pictures before and after the experiment were observed and compared. The values of amplitude, phase, resonance frequency, and dissipation were acquired in dry and water environment. The main evaluated QCM parameters were changes in resonance frequency ( $\Delta f$ ) and simultaneous changes in QCM energy dissipation ( $\Delta D$ ), corresponding to changes in mass and morphology of the investigated sensor structure. Thereby we identified sensor assay build up, its functioning in dry and water conditions as well as potential issues such as partial release of nanodiamonds during the chemical treatments.

**Keywords:** Quartz crystal microbalance (QCM); Nanodiamonds; Cortisol; Scanning electron microscopy (SEM); Frequency; Dissipation,

# Table of contents

Abstract.....	3
Table of contents.....	4
List of Abbreviations .....	5
List of Figures .....	6
<b>1. Introduction .....</b>	<b>7</b>
<b>2. Materials, methods and theory.....</b>	<b>13</b>
2.1. Materials.....	13
2.2 Fabrication of cortisol immunosensor .....	13
2.3 QCM theory and device.....	13
2.4 Measurement settings.....	17
<b>3. Results and discussion.....</b>	<b>19</b>
3.1. Optical characteristics of sensors after each functionalization .....	19
3.2. SEM pictures.....	20
3.3. QCM spectra example.....	20
3.4. Reproducibility.....	29
<b>4. Conclusion .....</b>	<b>30</b>
<b>References .....</b>	<b>31</b>
<b>Appendices.....</b>	<b>37</b>

# List of Abbreviations

<b>Ab</b>	Antibody of cortisol
<b>ACTH</b>	Adrenocorticotrophic hormone
<b>AFM</b>	Atomic force microscopy
<b>Ag</b>	Antigen
<b>BSA</b>	Bovine serum albumin
<b>CNC</b>	Cellulose nanocrystal
<b>Cortisol</b>	$C_{21}H_{30}O_5$ , hydrocortisone
<b>DNA</b>	Deoxyribonucleic acid
<b>RNA</b>	Ribonucleic acid
<b>DND</b>	Detonation nanodiamond
<b>EDC</b>	1-(3-Dimethylaminopropyl)-3-ethylcarbodiimide hydrochloride
<b>ELISA</b>	Enzyme linked immunosorbent assays
<b>HPA</b>	Hypothalamic–pituitary–adrenal
<b>HPLC</b>	High performance liquid chromatography
<b><math>KH_2PO_4</math></b>	Potassium phosphate monobasic
<b><math>K_2HPO_4</math></b>	Di-potassium hydrogen phosphate
<b>LSPR</b>	Localized surface plasmon resonance
<b>NDs</b>	Nanodiamonds
<b>NHS</b>	N-Hydroxysuccinimide
<b>PBS</b>	Phosphate buffer saline
<b>QCM</b>	Quartz crystal microbalance
<b>RIA</b>	Radioimmunoassay
<b>SEM</b>	Scanning electron microscopy
<b>SLBs</b>	Supported lipid bilayers
<b>SPR</b>	Surface plasmon resonance

# List of Figures

**Fig. 1.1** *Various bio-fluids used for cortisol estimation.*

**Fig. 1.2** *Molecular structure of Cortisol ( $C_{21}H_{30}O_5$ ).*

**Fig. 1.3** *Functional groups distributed on pristine ND surfaces.*

**Fig. 2.1** *Photograph of QCM experimental setup.*

**Fig. 2.2** (A) *Schematic representation of QCM-D plots.*

(B) *Representative  $\Delta D$ - $\Delta f$  plot signatures for cell adhesion on sensor surfaces*

**Fig. 2.3** *Standard design of QCM-Q1.*

**Fig. 2.4** *Standard design of Qsense sensor.*

**Fig. 2.5** *The software of Real-Time openQCM GUI-2.1.*

**Fig. 2.6** *Schematic presentation of the immunosensor fabrication.*

**Fig. 2.7** *Pictures of 10 microliters and 25 microliters of DND solutions of different concentrations originally and after repeated exposure to water and drying.*

**Fig 3.1.** *Pictures of QCM functional layers: Au, DND, EDC+NHS, Antibody, BSA, Antigen (100 nM).*

**Fig. 3.2** (A). *SEM images of bare sensor, 2% DND, 10% DND at 1  $\mu$ m.*

(B). *SEM images of 1  $\mu$ m at different concentrations of antigen.*

**Fig 3.3.1** *Amplitude in dry condition.*

**Fig 3.3.2** *Amplitude in water condition.*

**Fig 3.3.3** *Phase in dry condition.*

**Fig 3.3.4** *Phase in water condition.*

**Fig 3.3.5** *Resonance frequency in dry1 condition.*

**Fig 3.3.6** *Resonance frequency in water condition.*

**Fig 3.3.7** *Dissipation in dry condition.*

**Fig 3.3.8** *Dissipation in water condition.*

**Fig 3.3.9** *Line chart of phase changes.*

**Fig 3.3.10** *Line chart of amplitude changes.*

**Fig 3.3.11** *Line chart of resonance frequency changes.*

**Fig 3.3.12** *Line chart of dissipation changes.*

**Fig 3.3.13**  *$\Delta f$  in dry1, water, dry2 conditions.*

**Fig 3.3.14**  *$\Delta D$  in dry1, water, dry2 conditions.*

# 1. Introduction

Quartz crystal microbalance (QCM) based sensors became popular and widely explored for biosensing because of their ease of use for high sensitivity analyses of masses and conformations of adsorbed biomolecules as well as possibility of real -time sensing of analyte and reaction kinetics in fluid cells. The proper and long-term stable functionalization of QCM sensor surfaces has been previously studied and discussed by academics as it is crucial for biosensor applications [1]. They proposed the idea of covering QCM with a diamond film, which due to its properties offers the possibility of obtaining a stable surface termination using standard chemical-physical methods, and investigated the adhesion of two proteins (bovine serum albumin and fibronectin) on diamond-coated QCM surfaces with different terminations.

In recent years QCM devices have been continuously updated and modern QCM devices offer excellent sensitivity and precision, capable of detecting mass changes in the nanogram range. This makes them ideal for studying thin films, surface interactions and molecular adsorption processes and can be used for a variety of applications such as monitoring the adsorption of nanoparticles and molecules, studying cellular interactions, and environmental sensing, as well as for drug discovery and material characterization in the pharmaceutical industry. Recent advances include the development of a QCM with dissipation monitoring (QCM-D), which provides additional information about the viscoelastic properties of the layer under study. This extends the range of applications for QCMs and increases the depth of analysis. QCM is increasingly being integrated with other analytical techniques such as ellipsometry, surface plasmon resonance and electrochemical methods to provide more comprehensive data and insights. Enhanced software tools for data analysis and interpretation have also been developed in software and data analysis, enabling researchers to more easily analyze complex datasets and gain greater insight into their experiments. There is a trend to make QCM equipment more compact and portable, allowing for measurements to be taken in situ and analyzed in real time in a variety of environments. The QCM market is growing, driven by increasing use in academic research and industrial applications. Continuous research and development have led to new discoveries and improvements in QCM technology.

Recent studies have shown the application of QCM in many areas, such as the role of the dissipation monitoring (QCM-D) technique in understanding the mechanism of supported lipid bilayers (SLBs) formation and its use in combination with other analytical techniques such as atomic force microscopy (AFM) and localized surface plasmon resonance (LSPR) [2]. QCM technique has also been indispensable for the quantitative analysis of the interaction between A $\beta$  peptides and lipid membranes. It provides a methodological basis for the classification of A $\beta$  binding properties, which is essential for understanding the mechanisms of Alzheimer's



disease at the molecular level [3]. QCM technology has also been used to create a sensitive and selective gas sensor array for the detection and classification of acetone, a key biomarker for diabetes. Combining QCM with a variety of sensing films and sophisticated analytical techniques demonstrates a promising approach to non-invasive disease detection through breath analysis [4].

As the measurement technology of QCMs continues to improve, more attention is being paid to the enhancement of QCM sensors. Since the quality and performance of the sensor is highly dependent on the additional sensitive layer, additional sensing layers need to be added to the surface of the QCM electrodes to improve the sensor performance including selectivity, sensitivity, response time and stability [5].

The QCM's advantages include its great sensitivity, real-time monitoring capabilities, and many applications in surface science, nanotechnology, and biosensing [6]. However due to its susceptibility to temperature changes and environmental influences, data interpretation requires careful analysis, which comes with a high cost of equipment and experimentation [7]. Nowadays, QCM is used in many different fields, such as surface science to study coating changes [8] and biosensors [9] that identify biomolecular interactions. Prospective developments include enhancing stability and sensitivity, including machine learning [10] and nanotechnology [11], and creating specialized QCM devices for particular uses. This sensor type's versatility stems from its ability to control a QCM's selectivity through the application of various coatings, which is one of its main advantages.

The QCM is based on the principle of piezoelectric effect [12]. In addition, it is constructed around a quartz crystal, electrodes, and an oscillating circuit. Upon application of an electrical potential, the crystal oscillates at its characteristic frequency [13]. Frequency shifts are caused by mass perturbations on the crystal surface, such as coatings or adsorbed molecules [14]. These frequency shifts act as an indicator to identify mass changes. Therefore, by measuring the change in the oscillation frequency of the crystal, the amount of substance adsorbed and the surface properties can be recognized. Typically, the biosensor for detection and analysis of a biological/biochemical reaction is an electrode consisting of quartz coated with metals like Au or Ti [15]. To achieve high sensitivity, selectivity, and stability for the biosensor, the surfaces must be modified appropriately by a specific bioreceptor for each type of biosensing [15].

The most commonly employed bioreceptors due to their high specificity and selectivity are antibodies, enzymes, DNA (Deoxyribonucleic acid), RNA (ribonucleic acid), cell receptors. As antibodies have a high specificity for identifying antigens, they are frequently utilized in biosensors. An antibody is a Y-shaped protein featuring specific regions that exhibit high selectivity for antigens. These regions form highly specific bonds with certain molecules or pathogens. An antigen, essentially an 'antibody generator', is a component that triggers the

generation of antibodies. It is recognized by the unique binding sites of antibodies. Antibodies are thus perfect for uses in environmental monitoring, food safety, and medical diagnostics. Enzymes are biological molecules that act as highly selective and specific catalysts. They are often used in biosensors to detect the presence of specific substrates, such as glucose in blood sugar monitoring devices. DNA and RNA can be used as bioreceptors due to their ability to specifically bind to complementary sequences. This property is exploited in genetic testing and molecular diagnostics. Cell receptors can be utilized in biosensor technology to detect the presence of various ligands. This is particularly useful in drug discovery and the study of cell signaling pathways.

QCM biosensors have been employed for the detection of a broad variety of biomolecules such as proteins [16], nucleic acids [17], peptides [18], oligonucleotides [19], and hormones [20]. QCM biosensors have been recognized for their reliability, cost-effectiveness, and sensitivity, and they utilize a label-free and real-time biorecognition mechanism. They have found applications in various fields, including biomedical applications, where they offer significant advantages [21].

In terms of parameters, QCM biosensors primarily observe frequency change ( $\Delta f$ ) and dissipation change ( $\Delta D$ ). Frequency change is related to the mass change on the sensor surface. When a biomolecule binds to the sensor surface, it causes a change in the mass, which in turn alters the resonance frequency of the quartz crystal. This frequency shift is proportional to the mass of the adsorbed biomolecule, allowing for quantitative analysis [22]. The dissipation change parameter is particularly useful for monitoring the viscoelastic and conformational characteristics of a sample. Furthermore, QCM with dissipation monitoring (QCM-D) has been utilized as a tool to monitor cell adhesion, cytotoxicity, cell viability, and other important phenomena in cells, showcasing its versatility in bioengineering and biomedical research [23].

One significant steroid hormone that is linked to negative health outcomes is cortisol. It also plays a significant role in stress psychobiology [24]. Extended periods of stress stimulate the adrenocorticotrophic hormonal (ACTH) system, which results in the adrenal cortex releasing cortisol hormones. Cortisol is the end product of the hypothalamic–pituitary–adrenal (HPA) axis, which is the main component of the human body's adaptive system to maintain regulated physiological processes under changing environmental factors [25]. Stress influences many other biomarkers, but the most important and possibly clinically useful biomarker for measuring and tracking stress is cortisol [26]. Blood pressure, glucose levels, and the metabolism of carbohydrates are all influenced by cortisol levels. Additionally, it supports the immune, endocrine, skeletal, cardiovascular, and renal systems' homeostasis [26,27,28,29].

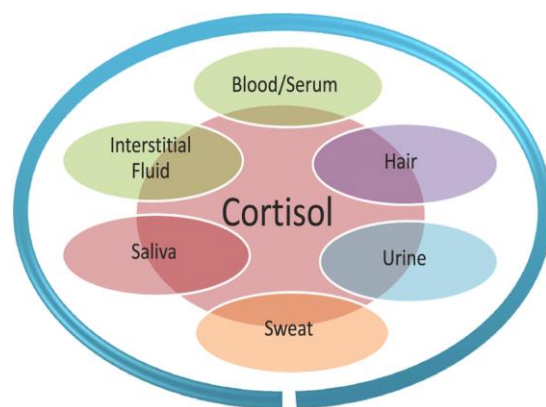


**Fig. 1.1** Various bio-fluids used for cortisol estimation [25].

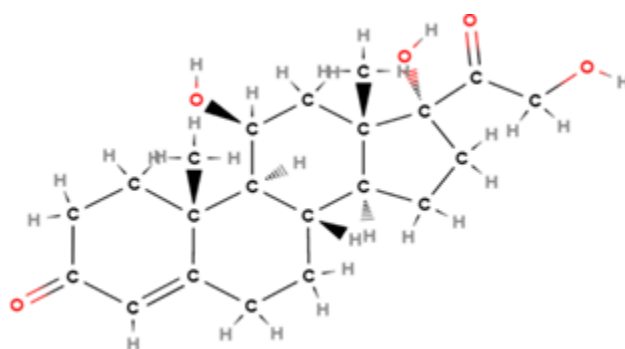


**Fig. 1.2** Molecular structure of Cortisol ( $C_{21}H_{30}O_5$ ).

There are many methods of detecting cortisol nowadays, such as surface plasmon resonance (SPR) [30,31], Enzyme linked immunosorbent assays (ELISA) [32], radioimmunoassay (RIA) [33] and electrochemical immunosensors [34].

For improving a biosensors sensitivity (the steepness of a slope of concentration calibration curve) and limit of detection (the lowest resolvable concentration of target molecule in analyte), the use of novel materials and nanomaterials for modifying the active sensor surface. These materials can often improve the sensor response by increasing its surface area by nanomorphology as well as provide new physical and chemical and charge transfer effects directly affecting the molecular sensing mechanism. The incorporation of new nanomaterials and nanodiamonds into biosensor technology marks a significant advancement in enhancing their sensitivity and limit of detection. These materials were selected because of their high surface-to-volume ratio, which increases target molecule interaction sites and enhances sensor responsiveness. Particularly nanodiamonds have special electrical qualities that are essential to biosensing mechanisms, such as redesigned bandgaps for effective charge transfer. Furthermore, their chemical stability and biocompatibility guarantee reliable and secure functioning in

intricate biological settings. These nanomaterials are adaptable for a range of applications because of their ability to be customized for the targeted detection of particular molecules. All things considered, the application of these cutting-edge nanomaterials in biosensors opens up new possibilities for developing more precise, sensitive, and trustworthy detection systems for a variety of applications, from environmental monitoring to medical diagnostics.

Diamond films have previously been used in QCM sensors with good experimental results. For example, V. Procházka et al. modified diamond-coated QCM (DQCM) with hydrogen and oxygen to control surface properties [1]. It was concluded that diamond-coated QCM sensors offer significant advantages in terms of sensitivity and specificity for protein detection, making them promising for a variety of biosensing applications. M. Varga et al. developed gas sensors based on QCM coated with nanocrystalline diamond (NCD) and observed that the NCD-coated QCM has higher sensitivity and better stability than the bare QCM [35].

In our research, we explored such possible benefits of nanodiamonds. We focused on using QCM for studying interaction between nanodiamonds, antibodies, and cortisol to better understand their function in biosensors. Diamond nanoparticles, within the framework of QCM experiments. Nanodiamonds, known for their exceptional chemical stability, biocompatibility, and unique optical properties, present a promising avenue for enhancing biosensor performance. In this study, we investigated the potential of nanodiamonds to improve the sensitivity and specificity of QCM-based detection systems. The large surface area and the ability to functionalize nanodiamonds could lead to improved binding efficiency and specificity when detecting target molecules such as antibodies and cortisol.

Detonation nanodiamonds (DNDs) carbon particles with a size of  $4 \pm 6$  nm, is one of the few commercially produced products that belongs to the family of nanocarbons, which also includes fullerenes, carbon nanotubes, graphene, globular nanocarbon, onions, and other structures [36]. More and more high-tech applications are using them, including polishing artificial crystals, modifying plastics and resins, creating wear-resistant coatings, and using them as greases and friction modifiers to change the rate at which surfaces wear [37,38]. The literature reports that different functional groups like alcohol, amine, amide, carboxylic acid, and carbonyl are naturally present on the surface of nanodiamonds [39,40]. Thereby, they can provide good interface for linking bioreceptors or adsorbing biomolecules directly [39,41]. Nanodiamonds (NDs) were also used for humidity sensors as part of a high-performance nanodiamond/cellulose nanocrystal (ND/CNC) composite-based acoustic humidity sensor [42]. NDs are particularly attractive for this application due to their large specific surface area, higher chemical stability, and mechanical modulus. They significantly optimized the humidity-sensitive performance of the sensors, improving their sensitivity and reducing humidity hysteresis. The unique properties of NDs make them a potent material for enhancing the capabilities of QCM humidity sensors.

DNDs may also enhance nanomorphology of the sensor surface and even facilitate charge transfer mechanism for complementary electrochemical sensing of cortisol. Their high surface area-to-volume ratio and rich surface chemistry enable effective surface modifications. This can lead to improved sensitivity and selectivity in cortisol detection, crucial for stress and health monitoring. The electrochemical properties of DNDs, combined with their biocompatibility, make them suitable for developing advanced biosensors for cortisol, offering potential for non-invasive and real-time monitoring in clinical and health applications.

This research may thus help expand nanodiamond applications in biosensing and explore their effectiveness in a QCM setup, thereby paving the way for more advanced, sensitive, and reliable biosensing technologies.

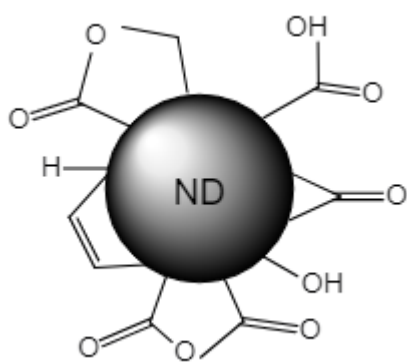


**Fig. 1.3** Functional groups distributed on pristine ND surfaces.

## 2. Materials, methods and theory

### 2.1. Materials

Potassium phosphate monobasic ( $\text{KH}_2\text{PO}_4$ ) solvent, di-potassium hydrogen phosphate ( $\text{K}_2\text{HPO}_4$ ) powder, N-Hydroxysuccinimide 98% (NHS), N-(3-Dimethylaminopropyl)-N'-ethylcarbodiimide hydrochloride (EDC), Bovine serum albumin (BSA), hydrocortisone (cortisol) (1 mg/1 mL methanole), were obtained from Sigma-Aldrich chemicals. Purified mouse monoclonal anti-cortisol-antibodi (5.605 mg/mL) was purchased from Abcam. Purified DND were supplied by NanoCarbon Research Institute Ltd. (particle size in the  $4.0\pm 0.8$  nm). PBS (pH 7.0, 0.05 M) was obtained by mixing of  $\text{K}_2\text{HPO}_4$  (2.336 g) and  $\text{KH}_2\text{PO}_4$  (1.577 g) in 50 mL of distilled water.

### 2.2 Fabrication of cortisol immunosensor

Firstly, 10  $\mu\text{L}$  of DND solution at 10% concentration was dropped on a clean QCM sensor and placed on a hot plate at  $40^\circ\text{C}$  allow it to be heated uniformly and dried completely after approximately 20 min. Next, 10  $\mu\text{L}$  of a mixture of EDC (400 mM) and NHS (100 mM) was dropped onto the dried surface and wait for 90 min before gently rinsing the surface with HPLC water. In the next step, 10  $\mu\text{L}$  of Ab (10  $\mu\text{g}/1\text{mL}$ ) solution was dropped on the surface of the modified QCM sensor and waited for 90 min at room temperature to immobilize the Ab. Excess Ab was then washed off the surface with HPLC water, after which 10 $\mu\text{L}$  of BSA (1%) solution continued to be added to the surface, and waited for 1h at room temperature, before being gently rinsed with HPLC water. This step is to make it block the non-specific binding sites and unbound functional groups on the Ab on the surface of QCM sensor. Then 10  $\mu\text{L}$  of 100 nM. Ag (8.92  $\mu\text{L}/5\text{mL}$ ) solution was dropped on top of the modified QCM sensor and waited for 90 min at room temperature before gently rinsing with HPLC water.

### 2.3 QCM theory and device

OpenQCM Q-1 device is the first open-hardware scientific instrument ready for soft matter research. It is an advanced quartz crystal microbalance, characterized by high sensitivity and precision in measurements. Equipped with real-time resonance frequency and Dissipation monitoring [14]. QCM is a surface-sensitive device that can measure molecular-scale events. It is also a sensitive and convenient method for examining mass changes at the boundary between

solid and liquid conditions. The piezoelectric effect is the foundation for the quartz crystal microbalance (QCM) sensor. This high-resolution mass sensing method has been applied extensively in a variety of domains, including surface chemistry, biochemistry, and biomedical engineering. Its sensitivity is at the picogram level [13].

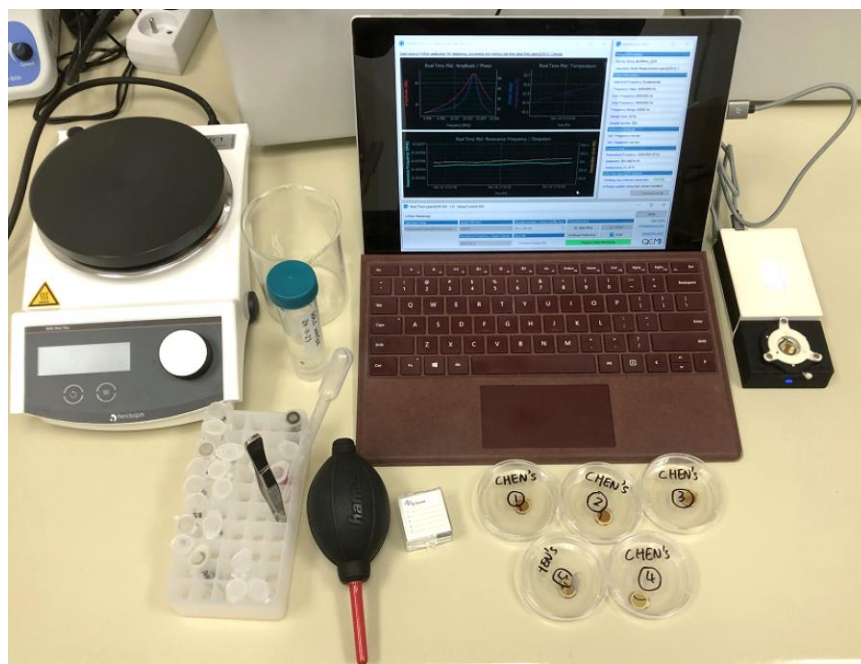


**Fig. 2.1** Photograph of our QCM experimental setup, showing QCM device, cables, computer, pipette, software, eppendorfs, sensors, blower, hot plate.

Measurements in three conditions of dry-water-dry were taken on the QCM sensor after each step of modification and four parameters were collected, namely: phase, amplitude, resonance frequency, and dissipation.

Amplitude reflects the oscillation intensity of the quartz crystal. In biosensors, amplitude changes can indicate mass alterations or surface interactions at the sensor interface. Frequency measures the rate of oscillation of the quartz crystal. In biosensors, a change in frequency directly corresponds to a mass change due to biomolecular adsorption or desorption. The phase angle in QCM indicates the nature of the mechanical load on the sensor. In biosensors, this can help in understanding the type of interaction (e.g., rigid or viscoelastic) between the sensor surface and the biomolecules. Dissipation measures energy loss in the system, indicating the viscoelastic properties of the adsorbed layer. In biosensors, it provides insight into the mechanical properties of biomolecular layers, essential for understanding molecular interactions and conformational changes.

It is derived that the quartz crystal's vibration amplitude changes in direct proportion to the change in its motional resistance [43]. Sauerbrey evidenced in 1959 that the frequency change

of an oscillating crystal is related to the surface adsorbed mass, where the linear relationship between the frequency change ( $\Delta f$ ) and the adsorbed mass ( $\Delta m$ ) is:

$$\Delta m = \frac{c}{n} \Delta f, \quad c = \frac{t_q \rho_q}{f_0},$$

where  $n$  is the harmonic number,  $\rho_q$  is density of quartz and equals  $-17.7 \text{ Hz ng/cm}^2$  for a 5-MHz crystal [44]. In order for the Sauerbrey relationship to hold, three conditions need to be met. Three requirements must be met: the mass adsorbed must be uniformly distributed throughout the active area of the crystal, rigidly adsorbed, and small in relation to the mass of the quartz crystal [44, 45].

In QCM measurements, the phase parameter is the change in phase of the oscillating signal, usually associated with a change in frequency, which can be used to measure the change in mass adsorbed on the surface of the crystal.

The QCM-D technology is highly sensitive and quantitative in measuring mass changes because it measures a frequency shift from the crystal's fundamental resonant frequency ( $\Delta f$ ) when a change in mass occurs at the surface interface or within the thin film. By recording variations in the energy dissipation factor ( $D$ ), QCM-D concurrently tracks the viscoelastic characteristics of the overlayer or thin film adsorbed to the quartz sensors (Fig. 2.2(A)). The amplitude of the crystal oscillation decays exponentially when the generator is turned off. By measuring the oscillation's amplitude as a function of time, one can determine the energy dissipation factor [46]. When there is a change in mass in either air or vacuum for a rigid layer ( $\Delta D = 0$ ), the frequency shift ( $\Delta f$ ) is proportional to the change in mass and can be measured using the Sauerbrey equation [44]. The equation proposed by Kanazawa and Gordon must be used to relate  $\Delta f$  to mass changes because biological processes occur in a liquid environment, where the Sauerbrey equation is no longer applicable [47].



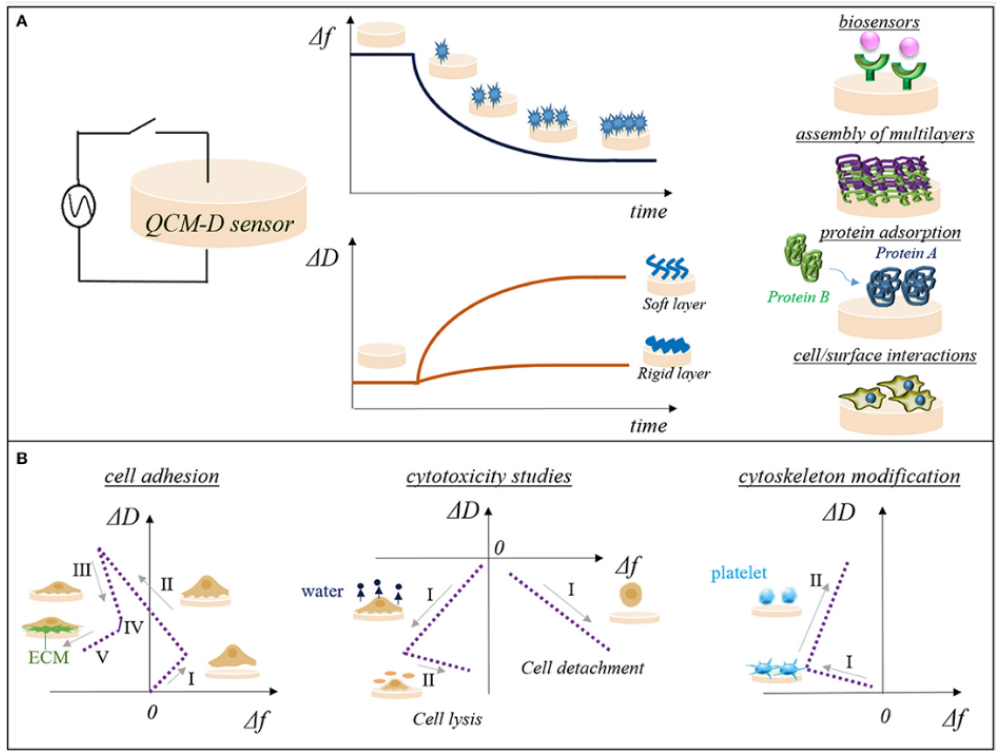


**Fig. 2.2** (A) Schematic representation of QCM-D plots reporting frequency factor ( $\Delta f$ ) and dissipation energy factor ( $\Delta D$ ) vs. time. (B) Representative  $\Delta D$ - $\Delta f$  plot signatures for cell adhesion on sensor surfaces (I-initial adhesion, II-formation of attachment points, III-cell spreading, IV-steady state of spread cells, V-production of ECM), cytotoxicity studies (left side: I-water release from cytoskeleton, II-cell lysis; right side: I-cell detachment) and cytoskeleton modification such as platelets activation (I-initial interactions among surface sensor and platelets, II-platelets spreading and pseudopodia formation) [48].

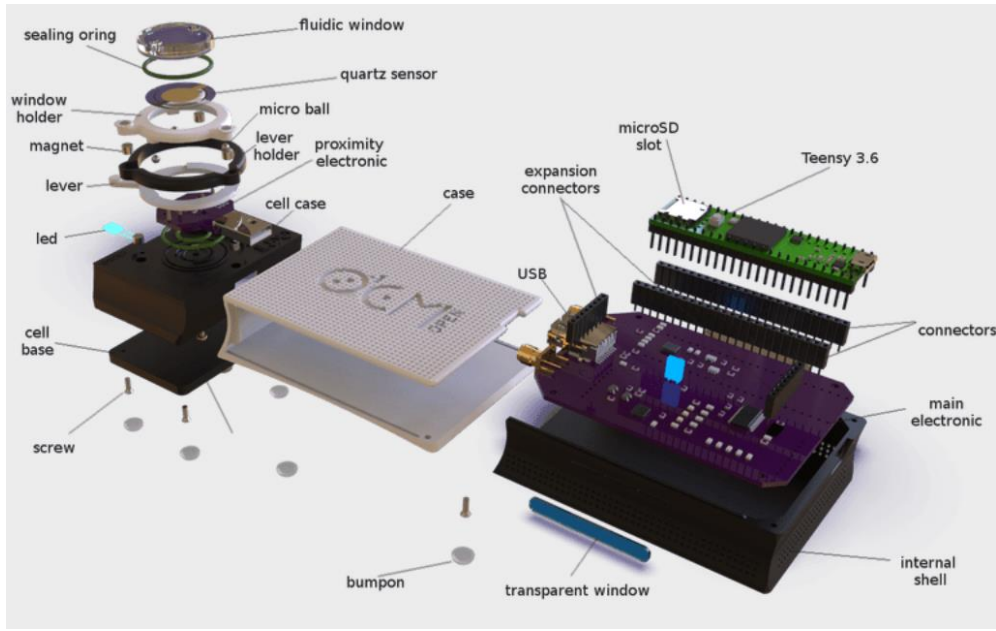


**Fig. 2.3** Standard design of QCM-Q1 [49].

## 2.4 Measurement settings

The sensor is at the heart of the QCM-D experiment. By using of QSX 301 comes in a box of 5 sensors from Biolinscientific company. The sensor's surface is gold (Au). The surface roughness was  $< 1$  nm RMS. It should be stored in a cool, dry place out of light. Stable baseline in air and deionized water in  $22\text{ }^{\circ}\text{C}$ . QSense sensors are 5 MHz to optimize the useful sensitivity, the sensing depth and the information required to quantify soft films.[49]

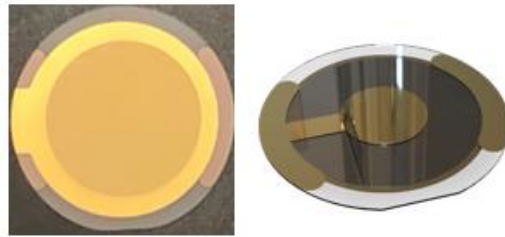


**Fig. 2.4** Standard design of Qsense sensor [50].

The Lorentzian resonance curve of the quartz is analyzed to determine the frequency, phase, and dissipation to be monitored during the measurement process. The software instructs the DDS synthesizer to obtain raw amplitude data from the gain/phase comparator and to passively excite the quartz crystal in the vicinity of its resonance frequencies. This configuration makes it possible to record the resonance curve in real time, which allows for the simultaneous monitoring of frequency and dissipation [51].

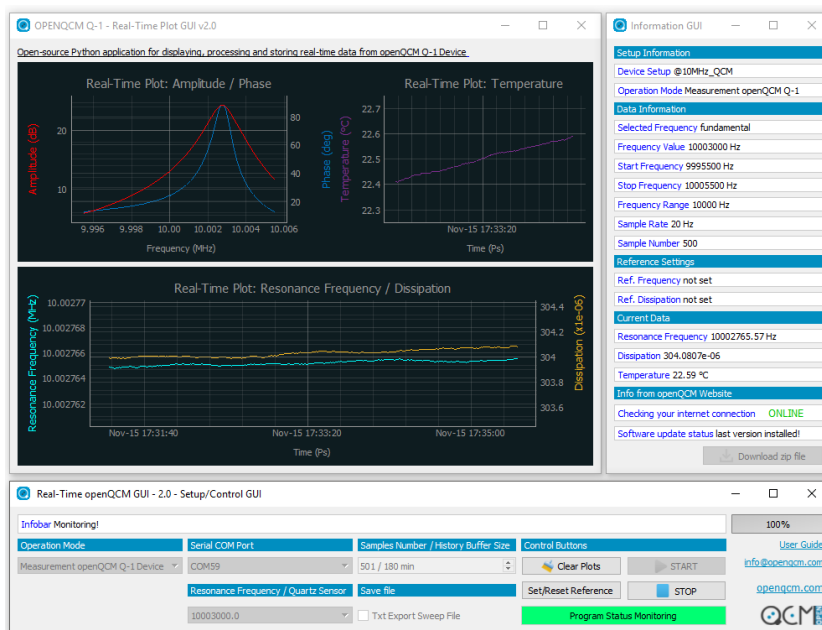


**Fig. 2.5** The software of Real-Time openQCM GUI-2.1 [51].

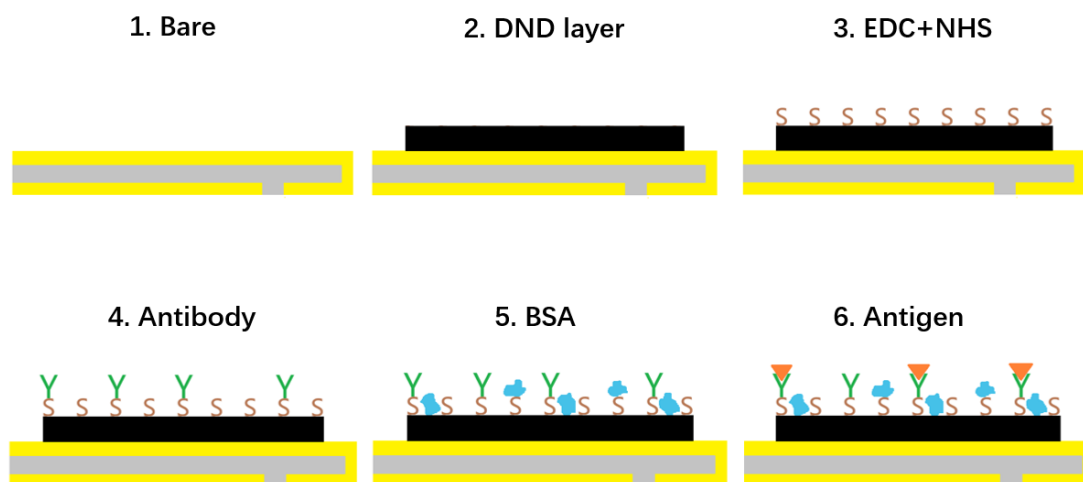


**Fig. 2.6** Schematic presentation of the immunosensor fabrication.

I also tested different volumes and concentrations of DND solutions on QCM sensors for dry1-water-dry2 experiments. Based on these experiments, we selected 10  $\mu\text{L}$  of 10% DND solution.

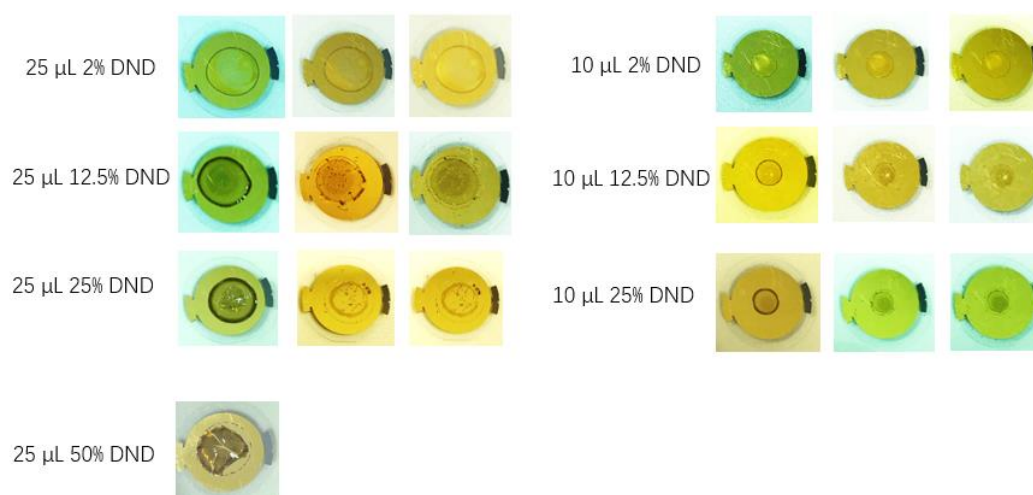


**Fig. 2.7** Pictures of 10 microliters and 25 microliters of DND solutions of different concentrations originally and after repeated exposure to water and drying.

### 3. Results and discussion

#### 3.1. Optical characteristics of sensors after each functionalization

Fig. 3.1 shows photographs of QCM in each functionalization steps Au, DND, EDC+NHS, Antibody, BSA, Antigen (100 nM). It can be observed from the optical pictures that during the DND step, the dry1 picture has a clear black edge and the black edge becomes lighter in colour in dry2. This means that DND lost some of it with water. After the reaction with the mixed solution of EDC and NHS, the colour of the black edges became lighter, and no significant changes were observed in dry1 and dry2 for this step. After adding antibody to the reaction, it can be observed that the black edges have disappeared and the edges have become transparent. After adding BSA to the reaction, no significant changes occurred. After adding Ag reaction can be observed that the circle loses its lustre and becomes a little thinner.

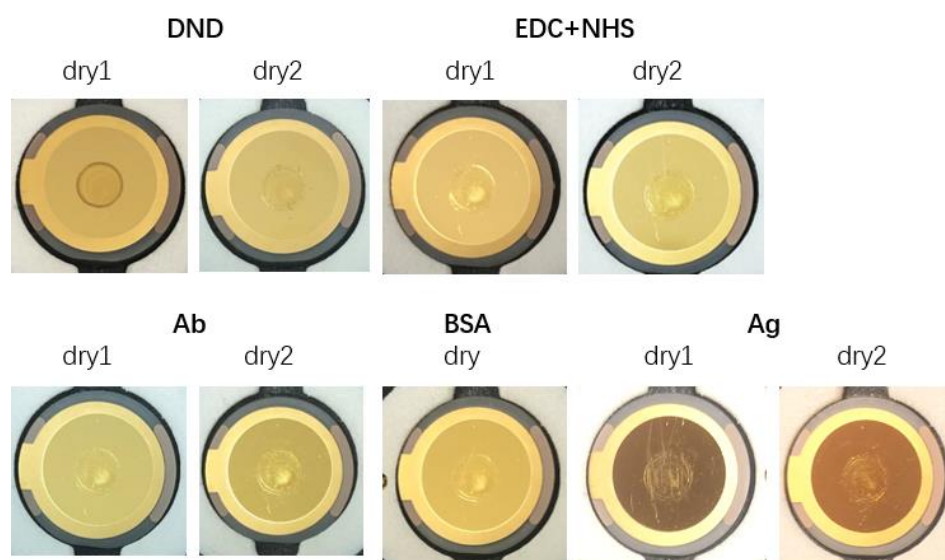


**Fig 3.1.** Pictures of QCM functional layers: Au, DND, EDC+NHS, Antibody, BSA, Antigen (100 nM).

### 3.2. SEM pictures

Figure 3.2 shows the results of Scanning Electron Microscopy (SEM) employed to examine the surfaces of a bare sensor and sensors treated with 2% and 10% DND at 1  $\mu\text{m}$ . In the SEM images of the bare sensor, a relatively uniform and clear surface morphology was observed. When observing the 2% and 10% of DND solutions on the SEM images, a clear difference in their nanoparticle morphology as well as the compact layer can be seen, where the 10% DND solution looks a bit more. This suggests that the deposition of DND on the sensor surface increases with the concentration of DND. SEM images at 1  $\mu\text{m}$  under different concentrations of antigen demonstrated significant morphological changes. With increasing antigen concentration, the number and density of these bright dots significantly increased, possibly due to the cumulative effect of the antigen on the sensor surface. The proliferation of these dot-like features suggests a more intense interaction of the antigen with the sensor surface.

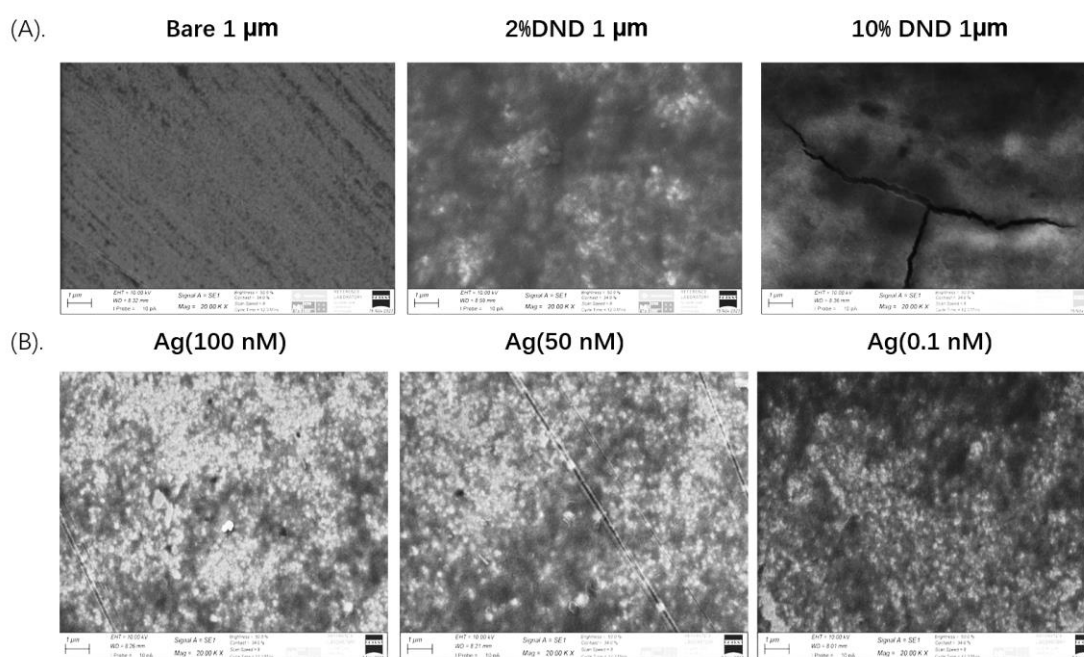


**Fig. 3.2 (A).** SEM images of bare sensor, 2% DND, 10% DND at 1  $\mu\text{m}$ .

**(B).** SEM images of 1  $\mu\text{m}$  at different concentrations of antigen.

### 3.3. QCM spectra example

In the following Figures there are spectral plots as well as time dependencies of frequency, phase, resonance frequency, and dissipation obtained as raw data from the software in dry and water environments, respectively. They show the shift and change of each of the four parameters as well as good temporal stability and low noise of the data.

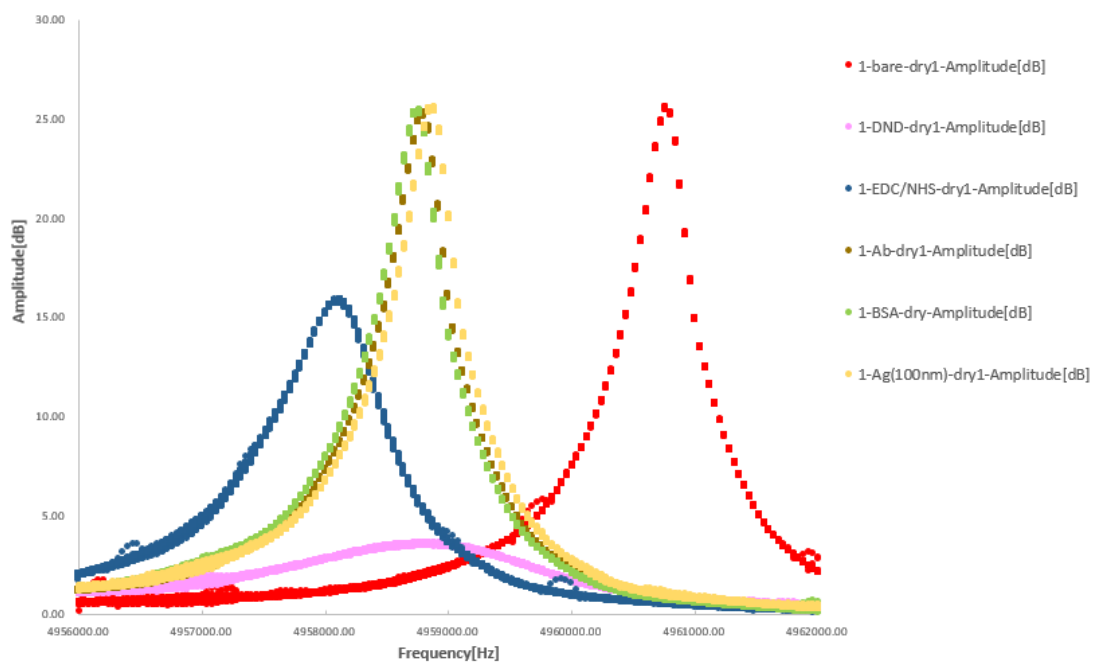


**Fig 3.3.1** Amplitude in dry condition.

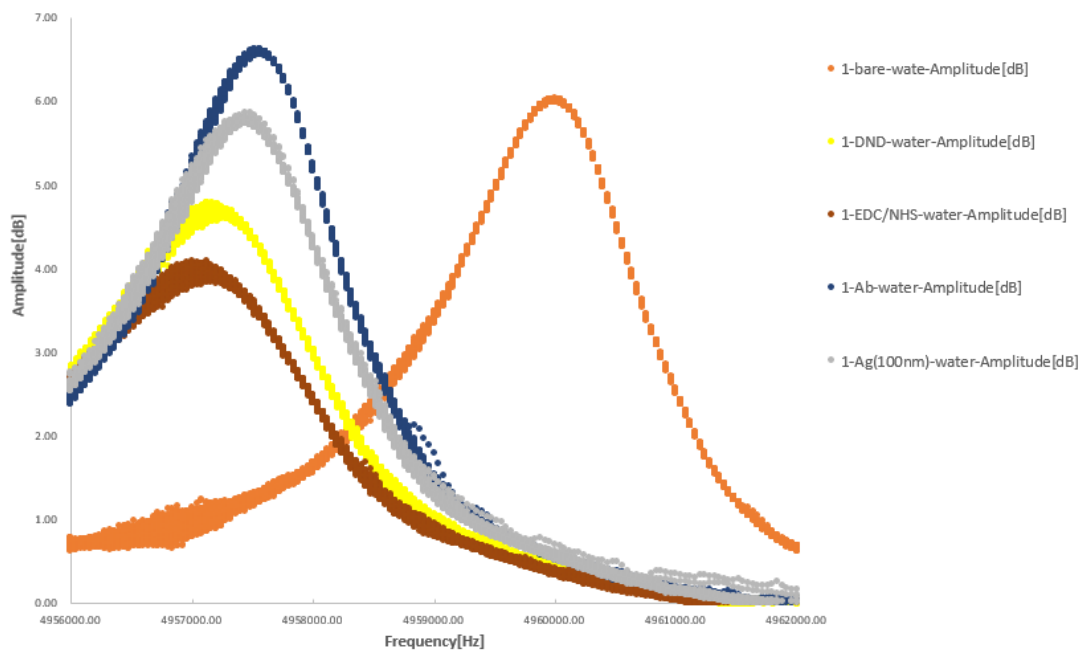


**Fig 3.3.2** Amplitude in water condition.

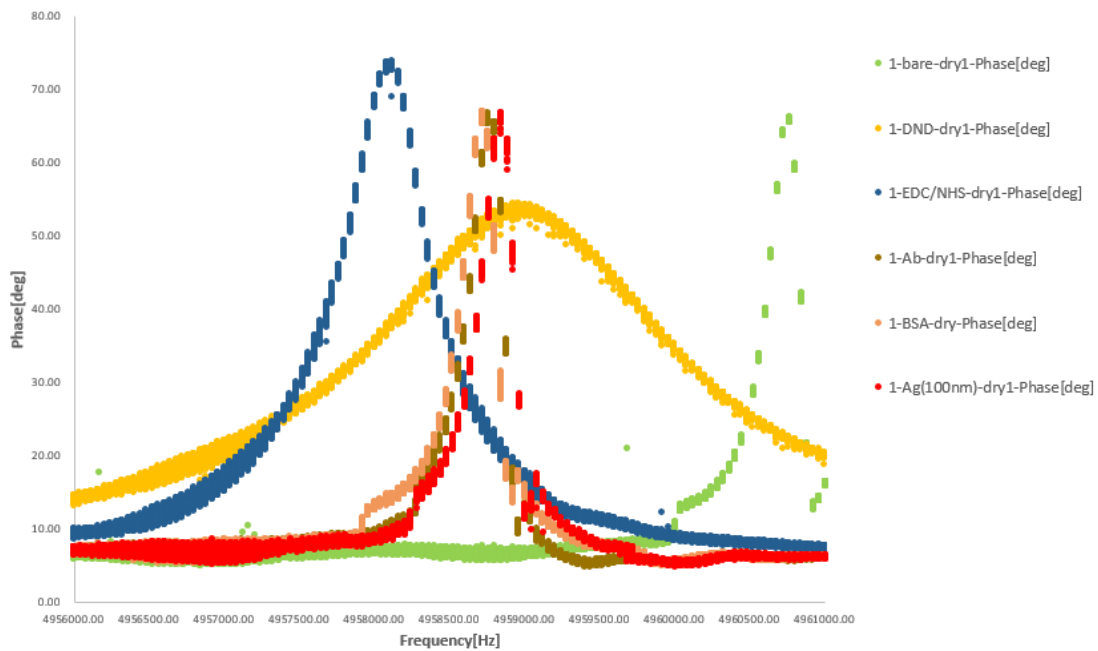


**Fig 3.3.3** Phase in dry condition.

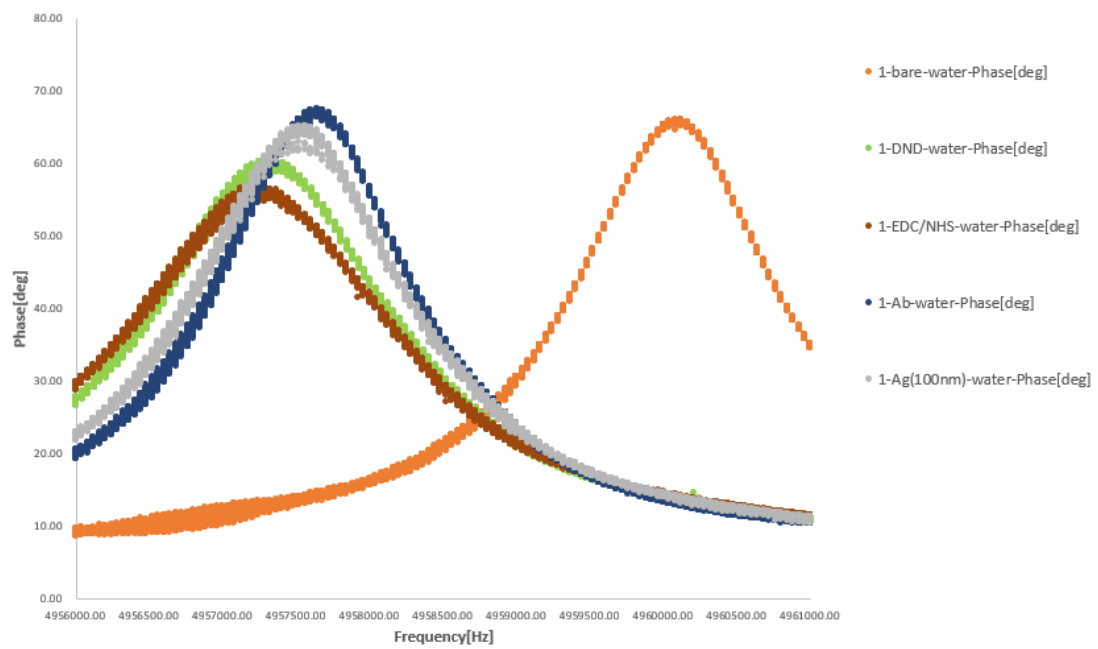


**Fig 3.3.4** Phase in water condition.

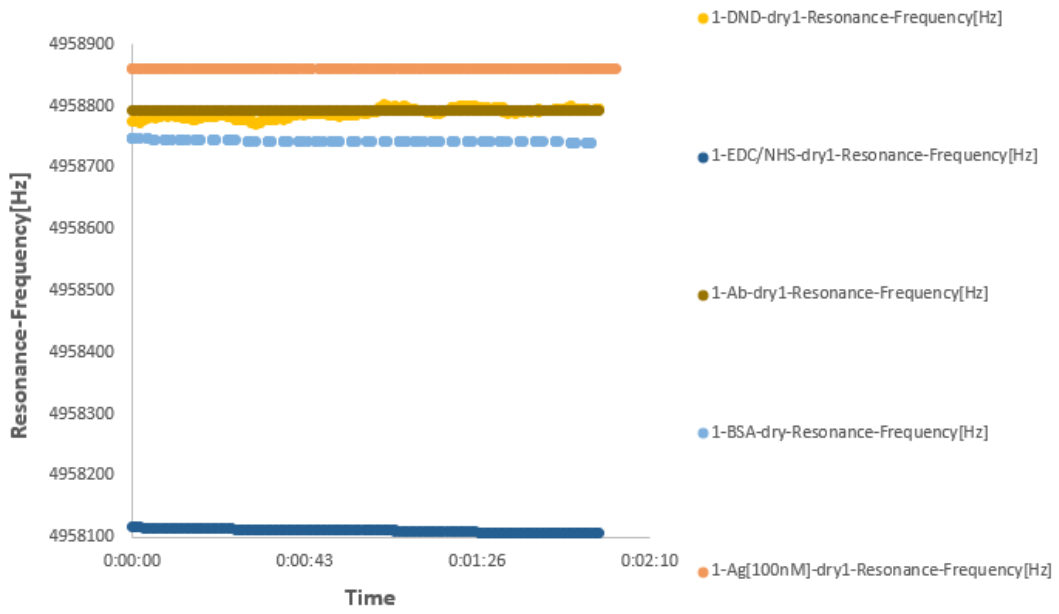


**Fig 3.3.5** Resonance frequency in dry1 condition.

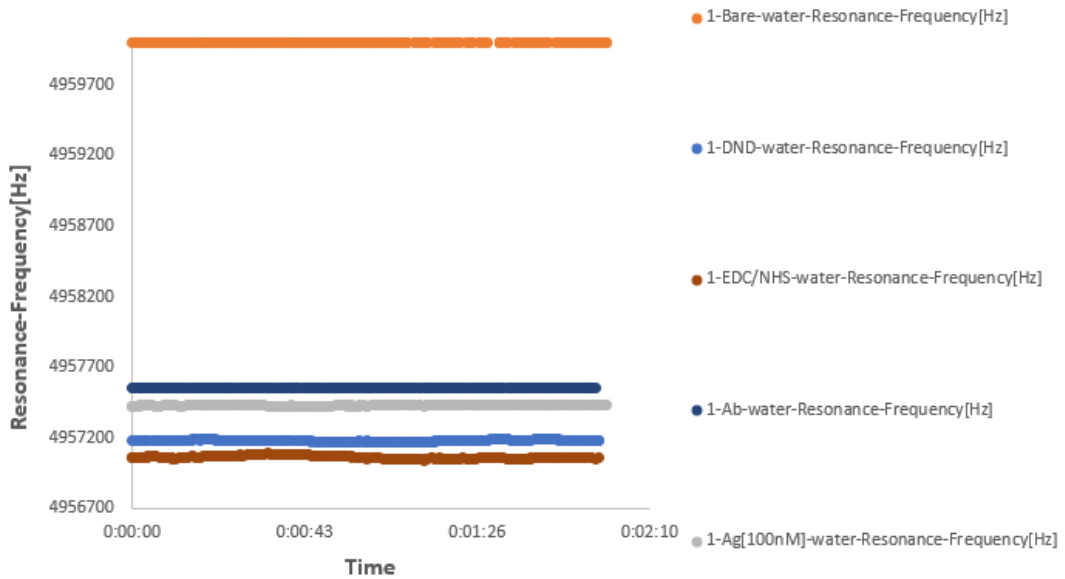


**Fig 3.3.6** Resonance frequency in water condition.



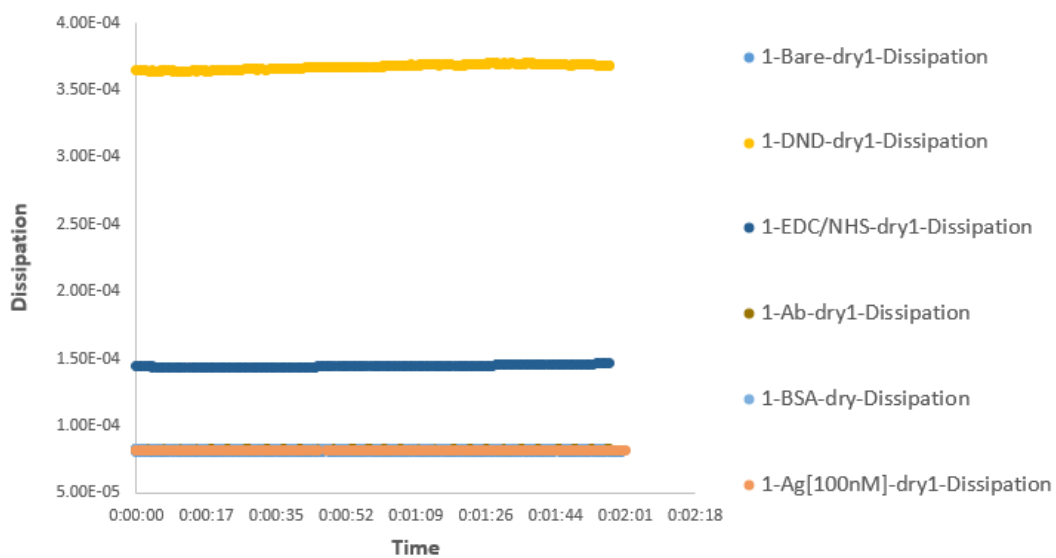


**Fig 3.3.7** Dissipation in dry condition.

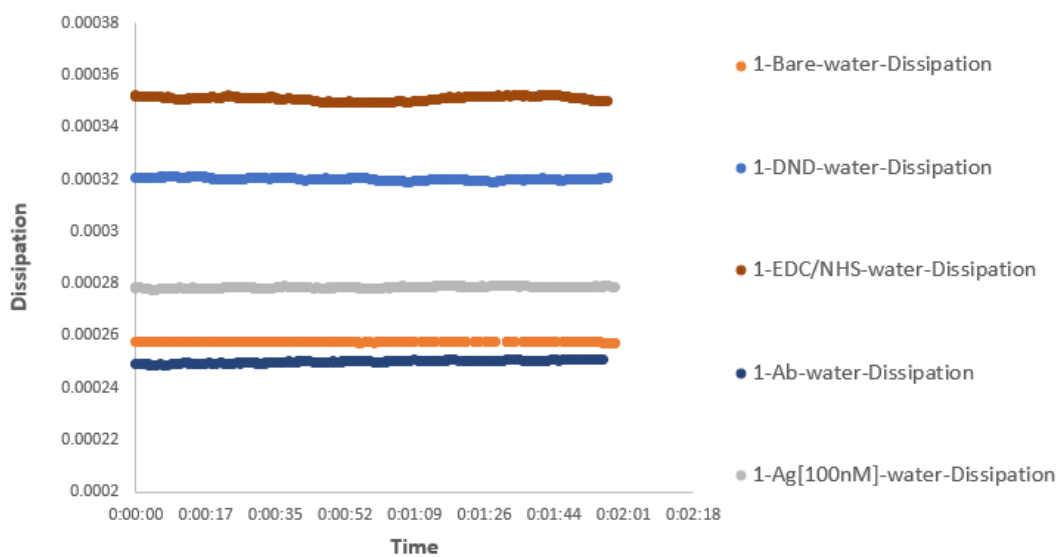


**Fig 3.3.8** Dissipation in water condition.

From the experimental raw data illustrated in the Figures above, we extracted dependency of characteristic QCM parameters on the functionalization steps of the sensor assay. The Figures below show line plots of the four parameters in both water and dry environments.

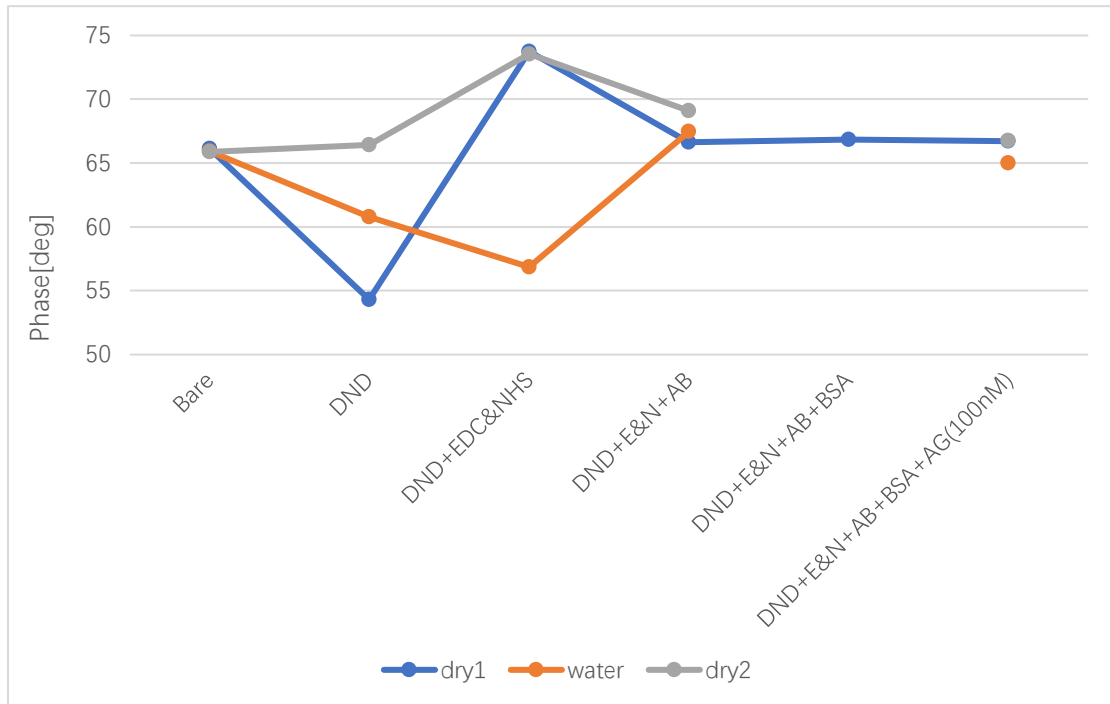


**Fig 3.3.9** Line chart of phase changes.

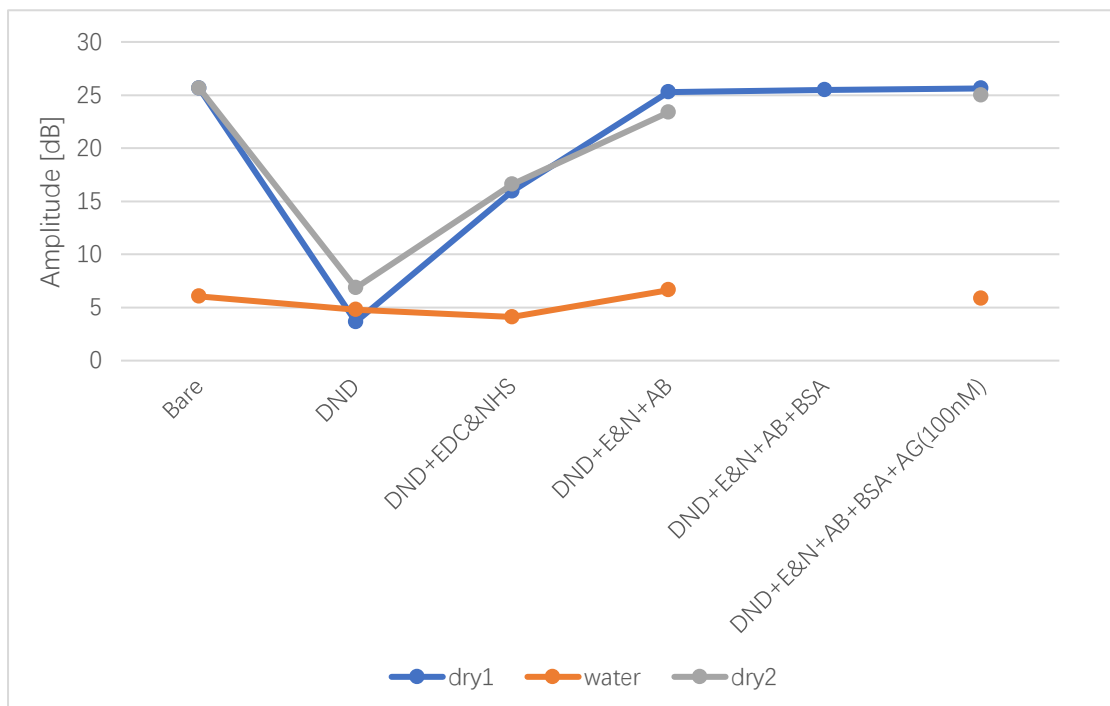


**Fig 3.3.10** Line chart of amplitude changes.

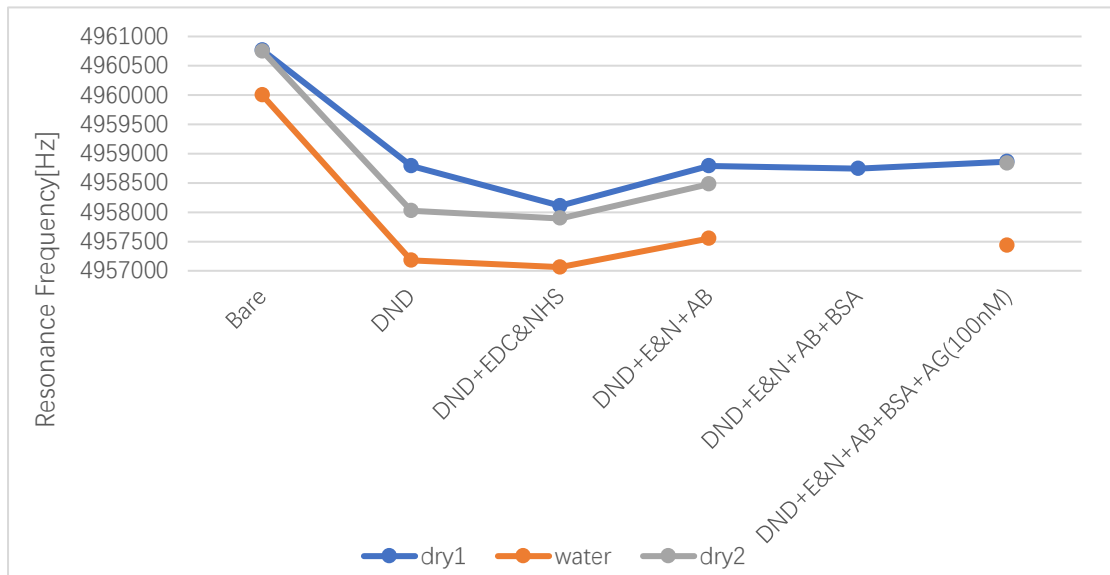


**Fig 3.3.11** Line chart of resonance frequency changes.

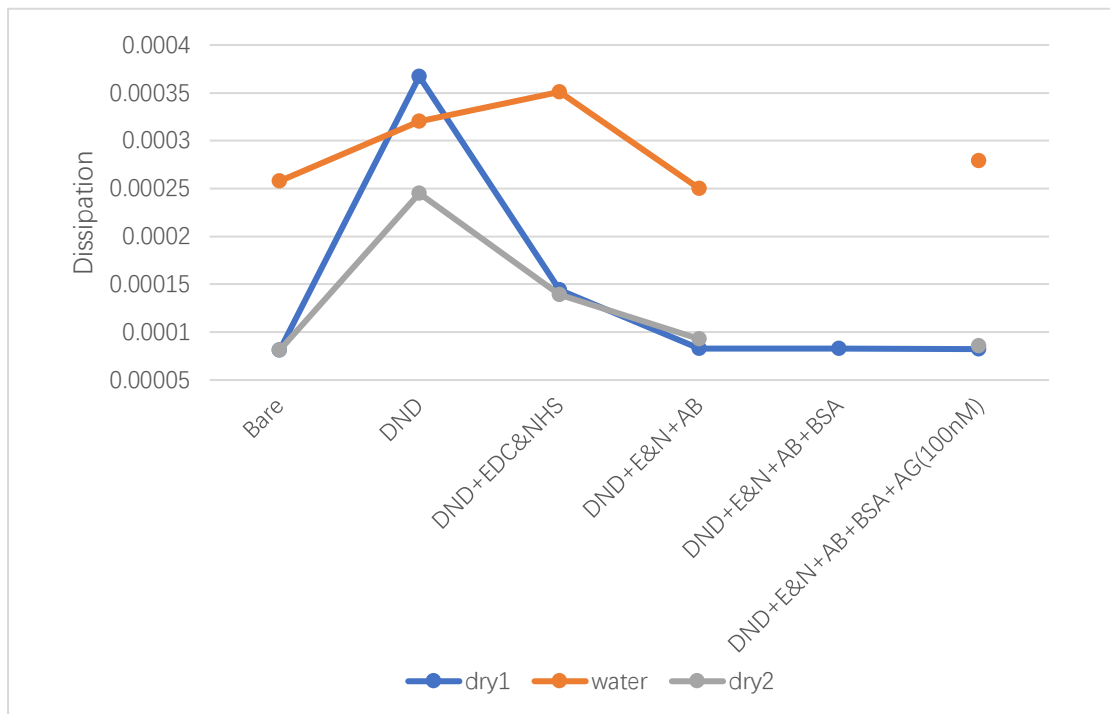


**Fig 3.3.12** Line chart of dissipation changes.

The observation of the above data shows that the phase increases significantly after the addition of the mixed solution of NHS and EDC, and then the phase value decreases significantly after the addition of Ab solution for the reaction, and the phase remains basically unchanged during the subsequent two-step reaction process with BSA and Ag solutions. The amplitude increased at each step of the operation after the addition of NHS and EDC.

Resonance frequency refers to the natural oscillation frequency of a quartz crystal oscillator when it is not adsorbed or attached to a substance. This frequency is one of the characteristics of quartz crystals. When there is no external mass attached to the surface of the quartz crystal, it will oscillate at its intrinsic resonance frequency. When a substance is adsorbed or attached to the surface of a quartz crystal, its mass changes, thus affecting its resonance frequency. By observing the change in resonance frequency, the change in mass adsorbed on the surface of the crystal can be inferred.

By observing the change in resonance frequency under dry and water conditions, it was seen that the value of resonance frequency increased significantly with the addition of further mixed solution of NHS and EDC. During the addition of Ab and BSA and Ag again, the resonance frequency remained basically unchanged. Dissipation usually refers to how much energy is dissipated from a crystal oscillation or how much the oscillating signal decays, and is sometimes referred to as the 'dissipation factor'. This dissipation is usually related to the adhesive or bonding properties of the adsorbed material. Therefore, the dissipation parameter is used in QCM as a measure to describe the degree of decay and energy loss of the crystal oscillation signal, which helps to provide a more comprehensive analysis and understanding of the adsorption process and the properties of the observed substance.

The most important evaluation step is to analyse differences after each each step. The following figures show the evaluation of  $\Delta f$  and  $\Delta D$  after each modification step. The frequency and dissipation data show significant effect of nanodiamond coating on QCM and that the series of reactions successfully immobilized Ab on the gold sensor, in agreement with the SEM images. By looking at the bar chart for  $\Delta f$ , it can also be seen that some of the nanodiamond was lost during the washing process, so it resulted in a negative value in the water. By looking at the error bar histogram of  $\Delta D$ , it can be seen that there is a significant change in the values for dissipation in the presence of EDC and NHS. In water as molecules are flowing in water, in dry environment the molecules collapse on the surface of the QCM sensor.

We still have problems with the concentration of nanodiamonds, we have also tried to optimize the concentration of Ag and present different amounts and structures under SEM observation (Fig. 3.2).

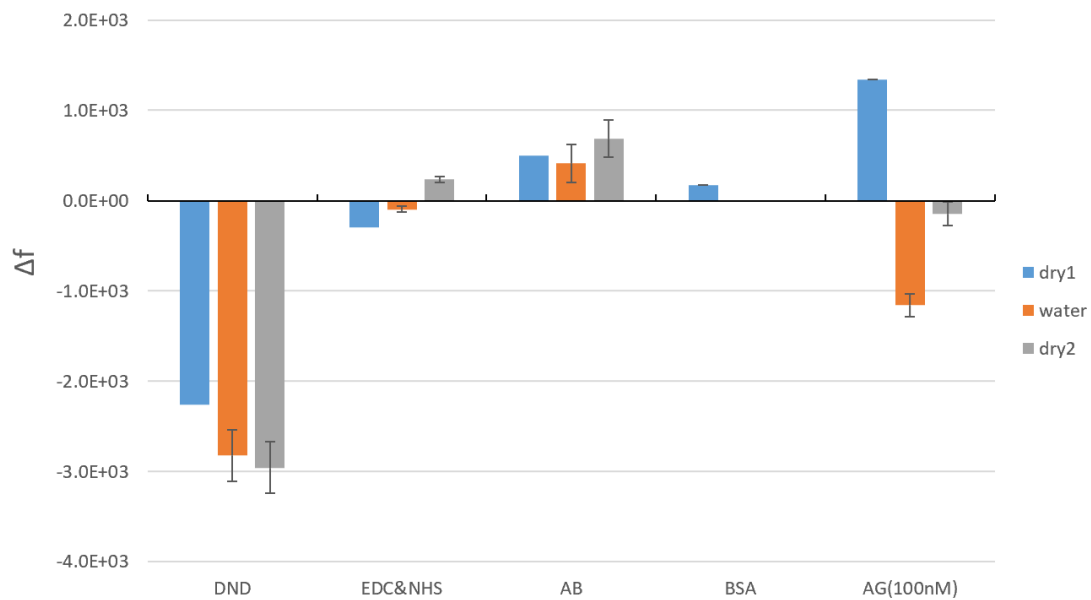


**Fig 3.3.13**  $\Delta f$  in dry1, water, dry2 conditions.

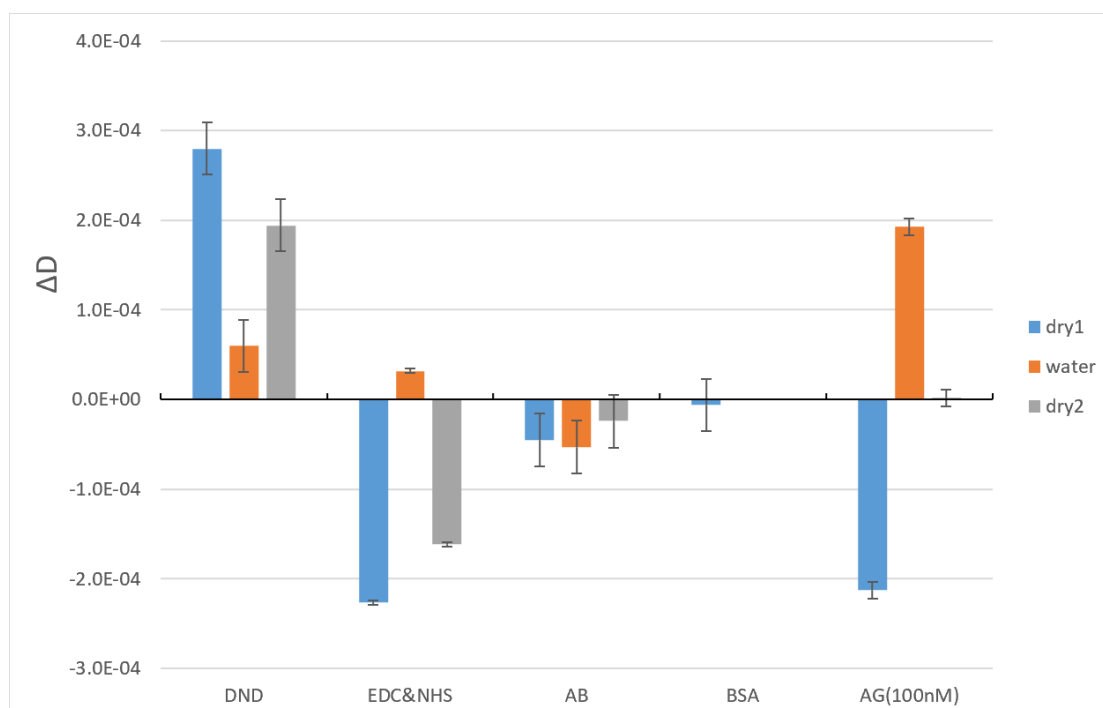


**Fig 3.3.14**  $\Delta D$  in dry1, water, dry2 conditions.

### 3.4. Reproducibility

I made three sets of data, all of which are in appendices. The data results are roughly similar with no obvious difference, which reflects the high consistency of the experimental results. Consistent results indicate both correct sensor function yet also that adhesion of nanodiamonds remains a problem for quantitative antigen analyses. Some nanodiamonds are most likely to be removed during the functionalization chemistries, thus  $\Delta f$  trend due to molecules is obscured by the opposite frequency increase due to nanodiamonds release. The bare sensor, in particular, exhibits notable stability and consistent performance throughout dry-to-wet-to-dry cycles.

## 4. Conclusion

We established a procedure and suitable parameters for the QCM sensor measurement and we finally chose a diluted 10% concentration of DND solution. During the cleaning process we used ethanol on the bare sensor for cleaning to avoid the influence of other impurities. HPLC water was used for cleaning after the reaction of dropping different substances on the sensor. This is because during the experiment it was found that when other types of water were used, a little salt might remain in it, which had an effect on the results of the experiment.

Too much concentration of DND was found to cause its poor adhesion on the surface of the sensor and peeling off during further processing. We also compared and observed the optical pictures after each functionalization step and the SEM pictures before and after the experiment. The values of amplitude, phase, resonance frequency, and dissipation were also compared between dry and water environment of the sensor. The results show that in the water environment, the dissipation values are larger than in the dry environment due to the floatation of molecules in the water. By observing the frequency values of dry1 and dry2 step, the decrease in the values is most likely still due to some loss of nanodiamonds adsorbed on the surface after the water step.

We also observed and compared  $\Delta f$  and  $\Delta D$ . They show consistently effect of molecular binding up to the antibody-antigen interaction. The decrease of the QCM frequency in some steps indicates the additional mass of nanodiamonds and molecules. Yet the increase of the frequency in some cases is most likely due to the release of some nanodiamonds from the surface, which we also proved with the optical images. This is most likely due to the chemicals weakening the adhesion between the DNDs. This masks the molecule-induced frequency shift, and the adhesion of DND to the QCM must be improved, e.g., by chemical grafting or surface chemical treatments (ethanol, plasma), because reducing the amount of DND is not enough. We also show the effect of various surface morphologies such as rough nanodiamond layers, molecular coatings, and rough antibodies in each functionalization step by observing  $\Delta D$ . By comparing the measurements in water and in the dry state, it was shown that in the dry state the molecules collapsed on the surface, showing lower dissipation due to making more rigid layer. In water environment the molecules tend to float, showing higher dissipation due to their flexibility. Thus, in general, measurements in water are more reliable for the sensor.

To sum up, the QCM technique has played a key role in elucidating DND interactions with molecules in the sensor assay. The QCM served as a platform for detecting the formation of Ab/ DND EDC NHS bioelectrode. This QCM-based immunoassay can be further improved by better adhesion of DNDs via chemical bonding and extended to the detection of other antigens and biological compounds.

# References

- [1] Procházka, V. et al. (2022) ‘Detection of globular and fibrillar proteins by quartz crystal microbalance sensor coated with a functionalized diamond thin film’, *Applied Surface Science*, 589, p. 153017. Available at: <https://doi.org/10.1016/j.apsusc.2022.153017>.
- [2] Bar, L. et al. (2023) ‘QCM-D Study of the Formation of Solid-Supported Artificial Lipid Membranes: State-of-the-Art, Recent Advances, and Perspectives’, *physica status solidi (a)*, 220(22), p. 2200625. Available at: <https://doi.org/10.1002/pssa.202200625>.
- [3] Shimanouchi, T. et al. (2023) ‘Classification of binding property of amyloid  $\beta$  to lipid membranes: Membranomic research using quartz crystal microbalance combined with the immobilization of lipid planar membranes’, *Biochimica et Biophysica Acta (BBA) - Proteins and Proteomics*, p. 140987. Available at: <https://doi.org/10.1016/j.bbapap.2023.140987>.
- [4] Rodríguez-Torres, M. et al. (2023) ‘Acetone Detection and Classification as Biomarker of Diabetes Mellitus Using a Quartz Crystal Microbalance Gas Sensor Array’, *Sensors*, 23(24), p. 9823. Available at: <https://doi.org/10.3390/s23249823>.
- [5] Demirtaş, Z. (2022) ‘Graphene oxide/calcium titanate composite preparation for humidity sensing by quartz crystal microbalance’. Available at: <http://hdl.handle.net/11527/24156>.
- [6] Naresh, V. and Lee, N. (2021) ‘A Review on Biosensors and Recent Development of Nanostructured Materials-Enabled Biosensors’, *Sensors*, 21(4), p. 1109. Available at: <https://doi.org/10.3390/s21041109>.
- [7] Lu, C. and Czanderna, A.W. (2012) ‘Applications of Piezoelectric Quartz Crystal Microbalances. Elsevier’. Available at: [https://books.google.com/books/about/Applications\\_of\\_Piezoelectric\\_Quartz\\_Cry.html?hl=zh-CN&id=cs9CXKuDbPQC](https://books.google.com/books/about/Applications_of_Piezoelectric_Quartz_Cry.html?hl=zh-CN&id=cs9CXKuDbPQC).
- [8] QCM biosensor with ultra thin polymer film - ScienceDirect (no date). Available at: <https://www.sciencedirect.com/science/article/abs/pii/S0925400504009086?via%3Dihub>.
- [9] Rodahl, M. et al. (1997) ‘Simultaneous frequency and dissipation factor QCM measurements of biomolecular adsorption and cell adhesion’, *Faraday Discussions*, 107(0), pp. 229–246. Available at: <https://doi.org/10.1039/A703137H>.
- [10] Rao, B.K. et al. (2021) ‘QCM Sensor-Based Alcohol Classification by Advance Machine Learning Approach’, in G.T.C. Sekhar et al. (eds) *Intelligent Computing in Control and*



Communication. Singapore: Springer (Lecture Notes in Electrical Engineering), pp. 305–320. Available at: [https://doi.org/10.1007/978-981-15-8439-8\\_25](https://doi.org/10.1007/978-981-15-8439-8_25).

[11] Nicolini, C., Bezerra, T. and Pechkova, E. (2012) ‘Protein nanotechnology for the new design and development of biocrystals and biosensors’, *Nanomedicine*, 7(8), pp. 1117–1120. Available at: <https://doi.org/10.2217/nmm.12.84>.

[12] Pohanka, M. (2021) ‘Quartz Crystal Microbalance (QCM) Sensing Materials in Biosensors Development’, *International Journal of Electrochemical Science*, 16(12), p. 211220. Available at: <https://doi.org/10.20964/2021.12.15>.

[13] Lucklum, R., & Eichelbaum, F. (2006, January 1) ‘Interface Circuits for QCM Sensors’, SpringerLink. Available at: [https://link.springer.com/chapter/10.1007/5346\\_023](https://link.springer.com/chapter/10.1007/5346_023).

[14] Marx K A. (2003) ‘Quartz Crystal Microbalance: A Useful Tool for Studying Thin Polymer Films and Complex Biomolecular Systems at the Solution–Surface Interface’, *Biomacromolecules*. Available at: <https://pubs.acs.org/doi/full/10.1021/bm020116i>.

[15] P j, J. et al. (2021) ‘Effective utilization of quartz crystal microbalance as a tool for biosensing applications’, *Sensors and Actuators A: Physical*, 331, p. 113020. Available at: <https://doi.org/10.1016/j.sna.2021.113020>.

[16] Chandrasekaran, N., Dimartino, S. and Fee, C.J. (2013) ‘Study of the adsorption of proteins on stainless steel surfaces using QCM-D’, *Chemical Engineering Research and Design*, 91(9), pp. 1674–1683. Available at: <https://doi.org/10.1016/j.cherd.2013.07.017>.

[17] Caruso, F. et al. (1997) ‘Quartz Crystal Microbalance Study of DNA Immobilization and Hybridization for Nucleic Acid Sensor Development’, *Analytical Chemistry*, 69(11), pp. 2043–2049. Available at: <https://doi.org/10.1021/ac961220r>.

[18] McCubbin, G.A. et al. (2011) ‘QCM-D fingerprinting of membrane-active peptides’, *European Biophysics Journal*, 40(4), pp. 437–446. Available at: <https://doi.org/10.1007/s00249-010-0652-5>.

[19] Ha, T.H. et al. (2004) ‘Influence of liquid medium and surface morphology on the response of QCM during immobilization and hybridization of short oligonucleotides’, *Biosensors and Bioelectronics*, 20(2), pp. 378–389. Available at: <https://doi.org/10.1016/j.bios.2004.02.027>.

- [20] Pali, M. et al. (2017) 'Detection of Fish Hormones by Electrochemical Impedance Spectroscopy and Quartz Crystal Microbalance', *Sensing and Bio-Sensing Research*, 13, pp. 1–8. Available at: <https://doi.org/10.1016/j.sbsr.2017.01.001>.
- [21] Rossini, P. et al. (2003) 'Surfaces engineering of polymeric films for biomedical applications', *Materials Science and Engineering: C*, 23(3), pp. 353–358. Available at: [https://doi.org/10.1016/S0928-4931\(02\)00286-2](https://doi.org/10.1016/S0928-4931(02)00286-2).
- [22] March, C. et al. (2015) 'High-frequency phase shift measurement greatly enhances the sensitivity of QCM immunosensors', *Biosensors and Bioelectronics*, 65, pp. 1–8. Available at: <https://doi.org/10.1016/j.bios.2014.10.001>.
- [23] Haberal, E., Ugur, N. and Kocakulak, M. (2013) 'QCM biosensor for testing the inflammatory response to blood-contacting biomaterials', *Artificial Cells, Nanomedicine, and Biotechnology*, 41(3), pp. 222–226. Available at: <https://doi.org/10.3109/10731199.2012.716068>.
- [24] G. Abbiendi et al. (2021) 'A study of muon-electron elastic scattering in a test beam'. Available at: <https://iopscience.iop.org/article/10.1088/1748-0221/16/06/P06005/pdf>.
- [25] Recent advances in cortisol sensing technologies for point-of-care application - ScienceDirect (2013, October 17). Available at: <https://www.sciencedirect.com/science/article/abs/pii/S0956566313006787?via%3Dihub>.
- [26] Iqbal, T. et al. (2023) 'Cortisol detection methods for stress monitoring in connected health', *Health Sciences Review*, 6, p. 100079. Available at: <https://doi.org/10.1016/j.hsr.2023.100079>.
- [27] Gatti, R. et al. (2009) 'Cortisol assays and diagnostic laboratory procedures in human biological fluids', *Clinical Biochemistry*, 42(12), pp. 1205–1217. Available at: <https://doi.org/10.1016/j.clinbiochem.2009.04.011>.
- [28] Levine, A. et al. (2007) 'Measuring cortisol in human psychobiological studies', *Physiology & Behavior*, 90(1), pp. 43–53. Available at: <https://doi.org/10.1016/j.physbeh.2006.08.025>.
- [29] de Kloet, E. R., Joëls, M., & Holsboer, F. (2005, May 13). 'Stress and the brain: from adaptation to disease', *Nature Reviews Neuroscience*. Available at: <https://www.nature.com/articles/nrn1683>.

- [30] Frasconi, M., Mazzarino, M., Botrè, F., & Mazzei, F. (2009, July 10). Surface plasmon resonance immunosensor for cortisol and cortisone determination | Analytical and Bioanalytical Chemistry. Available at: <https://link.springer.com/article/10.1007/s00216-009-2914-6>.
- [31] Towards integrated and sensitive surface plasmon resonance biosensors: A review of recent progress - ScienceDirect (2007, July 20). Available at: <https://www.sciencedirect.com/science/article/abs/pii/S0956566307002710?via%3Dihub>.
- [32] Albar, W.F. et al. (2013) 'Human hair cortisol analysis: Comparison of the internationally-reported ELISA methods', *Clinical and Investigative Medicine*, pp. E312–E316. Available at: <https://doi.org/10.25011/cim.v36i6.20629>.
- [33] Sink, T. D., Lochmann, R. T., & Fecteau, K. A. (2007, July 24). 'Validation, use, and disadvantages of enzyme-linked immunosorbent assay kits for detection of cortisol in channel catfish, largemouth bass, red pacu, and golden shiners', *Fish Physiology and Biochemistry*. Available at: <https://link.springer.com/article/10.1007/s10695-007-9150-9>.
- [34] Li, F., Li, Y., Dong, Y., Jiang, L., Wang, P., Liu, Q., Liu, H., & Wei, Q. (2016, February 16). 'An ultrasensitive label-free electrochemical immunosensor based on signal amplification strategy of multifunctional magnetic graphene loaded with cadmium ions', *Scientific Reports*. Available at: <https://www.nature.com/articles/srep21281>.
- [35] Varga, M. et al. (2015) 'Quartz crystal microbalance gas sensor with nanocrystalline diamond sensitive layer', *physica status solidi (b)*, 252(11), pp. 2591–2597. Available at: <https://doi.org/10.1002/pssb.201552229>.
- [36] Dolmatov, V.Y. et al. (2020) 'Detonation nanodiamonds: new aspects in the theory and practice of synthesis, properties and applications', *Russian Chemical Reviews*, 89(12), p. 1428. Available at: <https://doi.org/10.1070/RCR4924>.
- [37] Dolmatov, V.Y. (2001) 'Detonation synthesis ultradispersed diamonds: properties and applications', *Russian Chemical Reviews*, 70(7), p. 607. Available at: <https://doi.org/10.1070/RC2001v070n07ABEH000665>.
- [38] Larionova, I. et al. (2006) 'Properties of individual fractions of detonation nanodiamond', *Diamond and Related Materials*, 15(11), pp. 1804–1808. Available at: <https://doi.org/10.1016/j.diamond.2006.07.016>.

- [39] Gruen, D.M., Shenderova, O.A. and Vul', A.Y. (2005) Synthesis, Properties and Applications of Ultrananocrystalline Diamond: Proceedings of the NATO ARW on Synthesis, Properties and Applications of Ultrananocrystalline Diamond, St. Petersburg, Russia, from 7 to 10 June 2004. Springer Science & Business Media. Available at: [https://books.google.cz/books?id=gV5Nqsbr-ugC&printsec=frontcover&hl=zh-CN&source=gbs\\_ViewAPI&redir\\_esc=y#v=onepage&q&f=false](https://books.google.cz/books?id=gV5Nqsbr-ugC&printsec=frontcover&hl=zh-CN&source=gbs_ViewAPI&redir_esc=y#v=onepage&q&f=false).
- [40] Shenderova, O.A., Zhirmov, V.V. and Brenner, D.W. (2002) 'Carbon Nanostructures: Critical Reviews in Solid State and Materials Sciences: Vol 27, No 3-4'. Available at: <https://www.tandfonline.com/doi/abs/10.1080/10408430208500497>.
- [41] Aramesh, M. et al. (2015) 'Surface charge effects in protein adsorption on nanodiamonds', *Nanoscale*, 7(13), pp. 5726–5736. Available at: <https://doi.org/10.1039/C5NR00250H>.
- [42] Chen, Q. et al. (2022) 'Nanodiamond/cellulose nanocrystals composite-based acoustic humidity sensor', *Sensors and Actuators B: Chemical*, 373, p. 132748. Available at: <https://doi.org/10.1016/j.snb.2022.132748>.
- [43] Zhang, C. and Feng, G. (1996) 'Contributions of amplitude measurement in QCM sensors', *IEEE Transactions on Ultrasonics, Ferroelectrics, and Frequency Control*, 43(5), pp. 942–947. Available at: <https://doi.org/10.1109/58.535498>.
- [44] Sauerbrey, G. (1959) 'Verwendung von Schwingquarzen zur Wägung dünner Schichten und zur Mikrowägung', *Zeitschrift für Physik*, 155(2), pp. 206–222. Available at: <https://doi.org/10.1007/BF01337937>.
- [45] Dixon, M. C. (n.d.). 'Quartz Crystal Microbalance with Dissipation Monitoring: Enabling Real-Time Characterization of Biological Materials and Their Interactions – PMC'. Available at: <https://www.ncbi.nlm.nih.gov/pmc/articles/PMC2563918/>.
- [46] Rodahl, M. et al. (1995) 'Quartz crystal microbalance setup for frequency and Q-factor measurements in gaseous and liquid environments', *Review of Scientific Instruments*, 66(7), pp. 3924–3930. Available at: <https://doi.org/10.1063/1.1145396>.
- [47] Kanazawa, K.Keiji. and Gordon, J.G. (1985) 'Frequency of a quartz microbalance in contact with liquid', *Analytical Chemistry*, 57(8), pp. 1770–1771. Available at: <https://doi.org/10.1021/ac00285a062>.

[48] Tonda-Turo, C., Carmagnola, I. and Ciardelli, G. (2018) 'Quartz Crystal Microbalance With Dissipation Monitoring: A Powerful Method to Predict the in vivo Behavior of Bioengineered Surfaces', *Frontiers in Bioengineering and Biotechnology*, 6. Available at: <https://www.frontiersin.org/articles/10.3389/fbioe.2018.00158>.

[49] 'openQCM Q-1 Design' (no date) Quartz Crystal Microbalance with Dissipation Monitoring: Open Source QCM-D. Available at: <https://openqcm.com/openqcm-q-1-design>.

[50] 'openQCM Technology' (no date) Quartz Crystal Microbalance with Dissipation Monitoring: Open Source QCM-D. Available at: <https://openqcm.com/technology>.

[51] openQCM Q-1 Software - Quartz Crystal Microbalance with Dissipation Monitoring: Open Source QCM-D (no date). Available at: <https://openqcm.com/openqcm-q-1-software>.

# Appendices

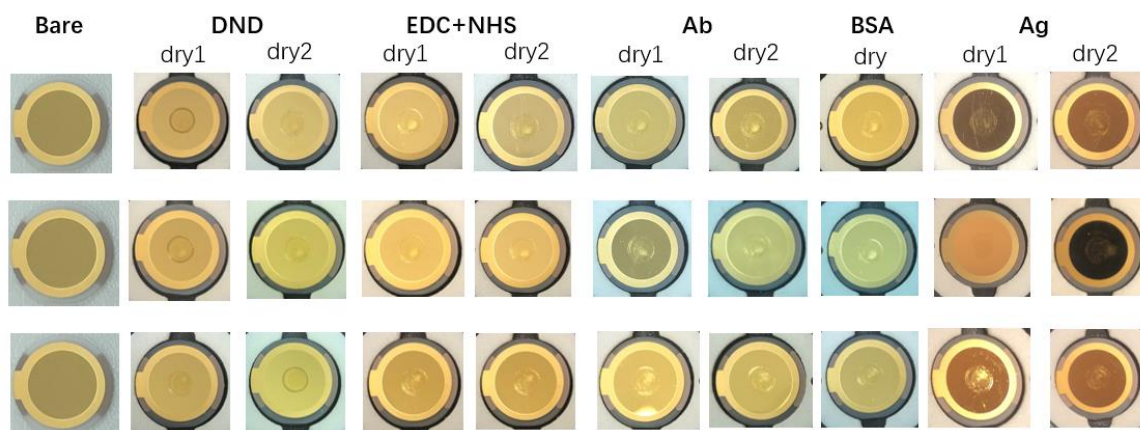


**Fig. A1.** A picture of QCM functional layers: Au, DND, EDC+NHS, Antibody, BSA, Antigen (100 nM) on three different sensors.

## DND+EDC/NHS+Ab+Ag(100nM)

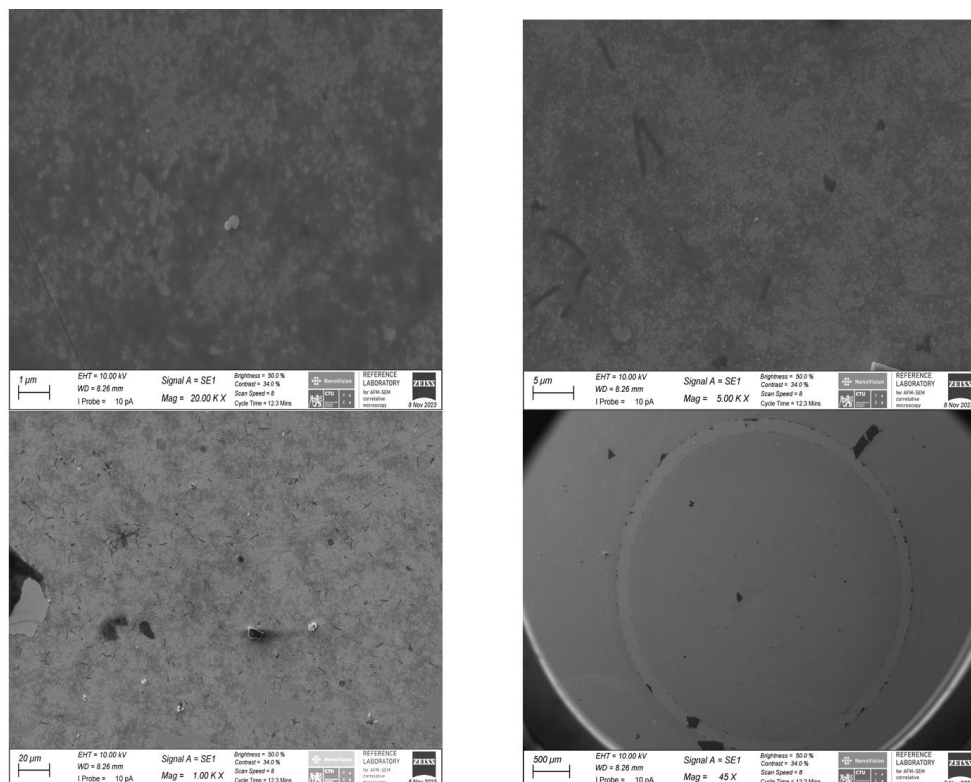


**Fig. A2.** SEM images after adding Ag (100 nM) at different magnifications.

DND+EDC/NHS+AB+AG(50nM)

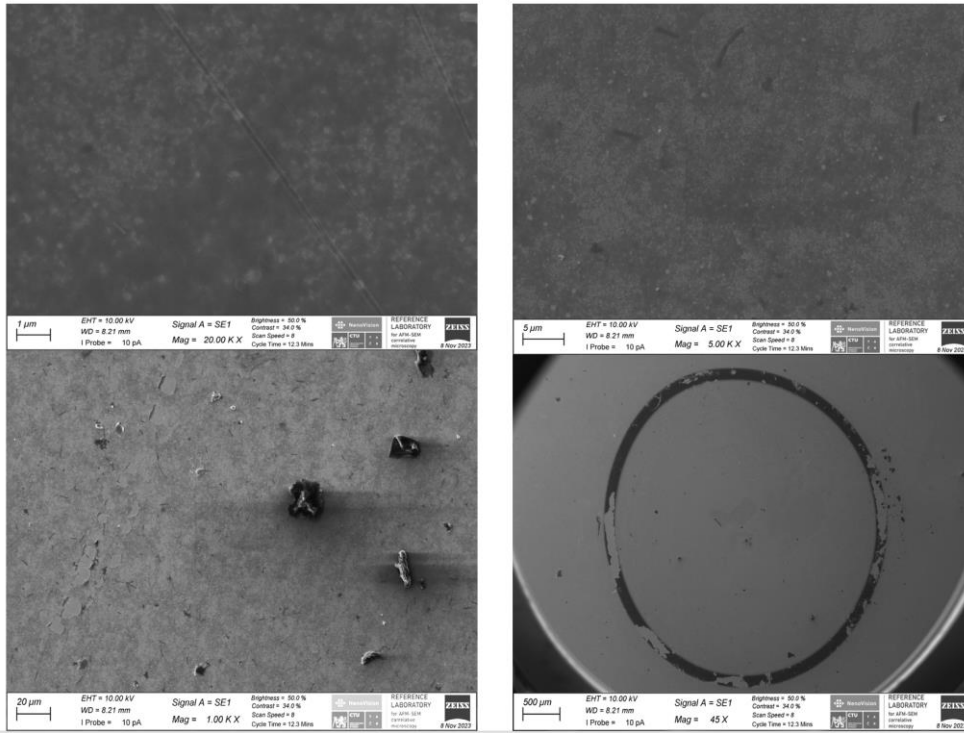


Fig. A3. SEM images after adding Ag (50 nM) at different magnifications.

DND+EDC/NHS+AB+AG(0.1nM)

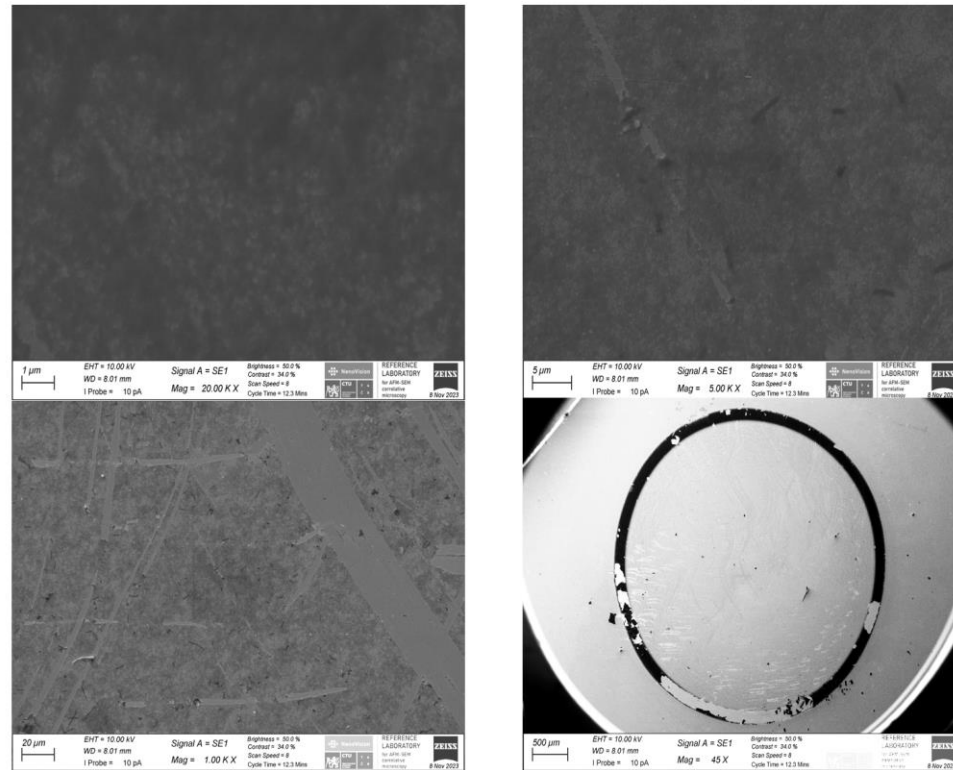
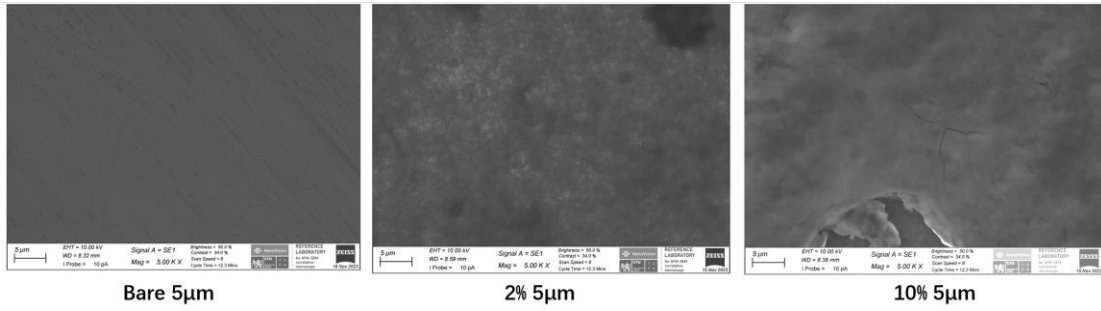
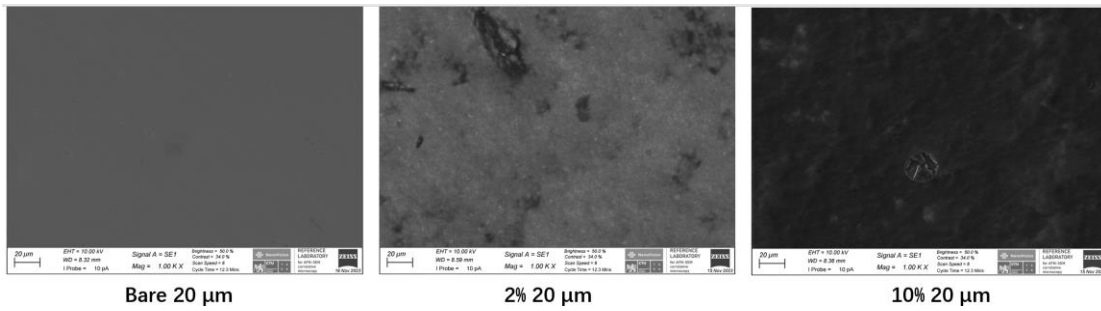


Fig. A4. SEM images after adding Ag (0.1 nM) at different magnifications.



**Fig. A5.** SEM images of bare sensor, 2% DND, 10% DND at 5 μm.



**Fig. A6.** SEM images of bare sensor, 2% DND, 10% DND at 20 μm.

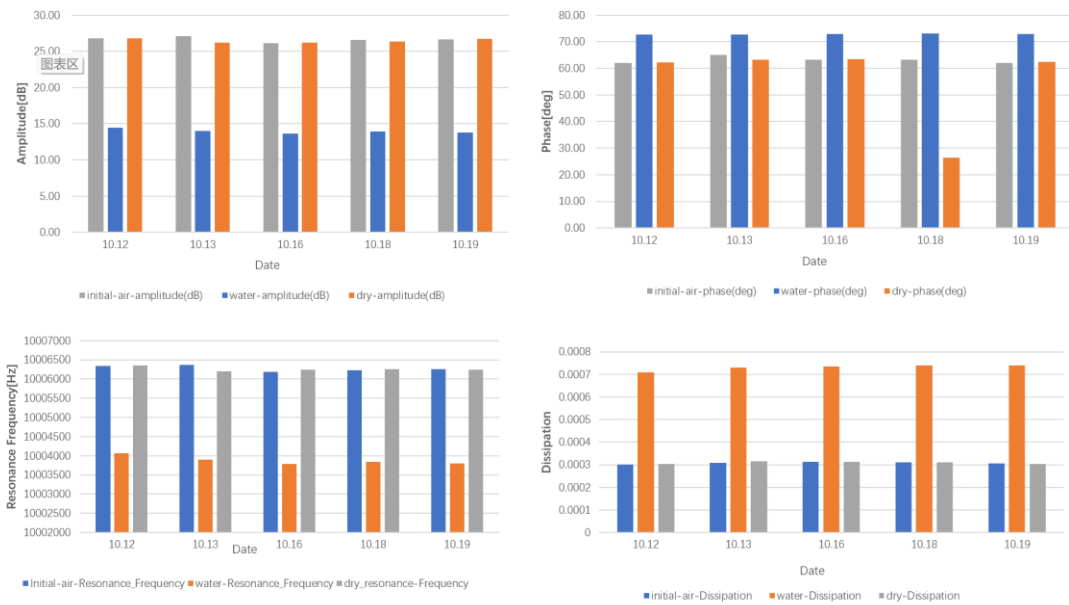


**Fig. B1.** Measurement of frequency, phase, resonance frequency and dissipation under Air-water-dry cycles with QCM sensors on different dates.



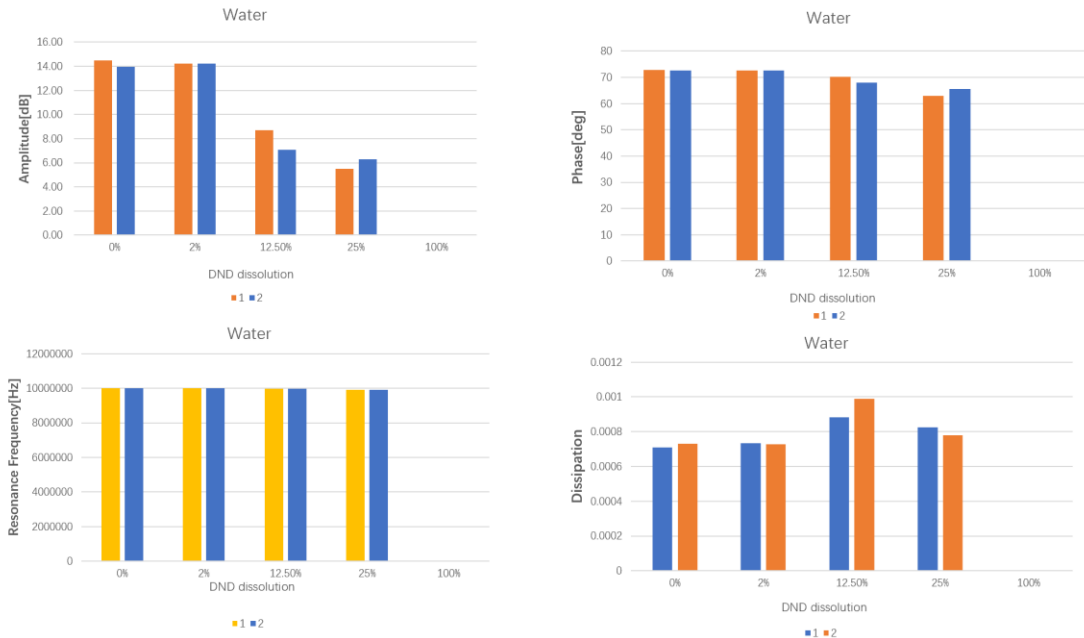


**Fig. B2.** Measurement of frequency, phase, resonance frequency and dissipation at different concentrations of DND solution in water.

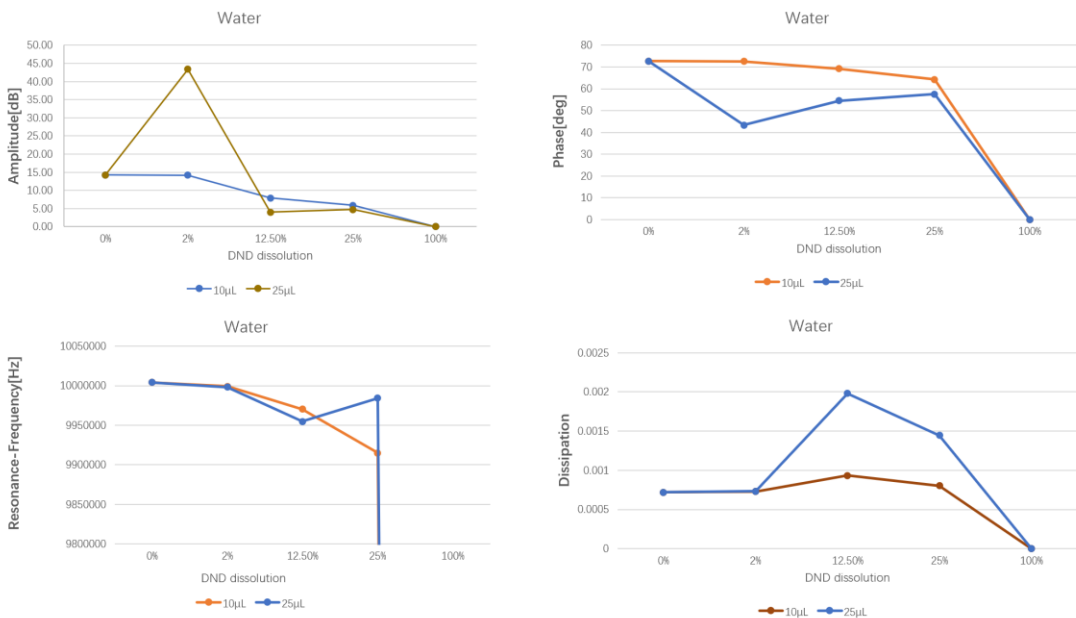


**Fig. B3.** Frequency, phase, resonance frequency and dissipation were measured in water with 10 µL and 25 µL of different concentrations of DND solution.

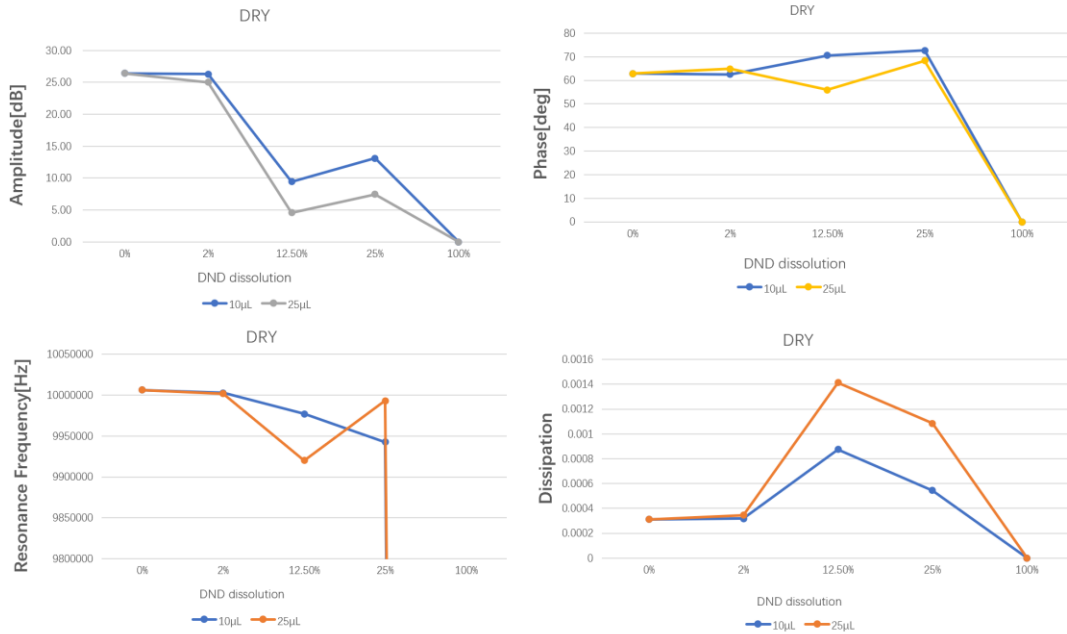


**Fig. B4.** Frequency, phase, resonance frequency and dissipation were measured in dry with 10  $\mu$ L and 25  $\mu$ L of different concentrations of DND solution.

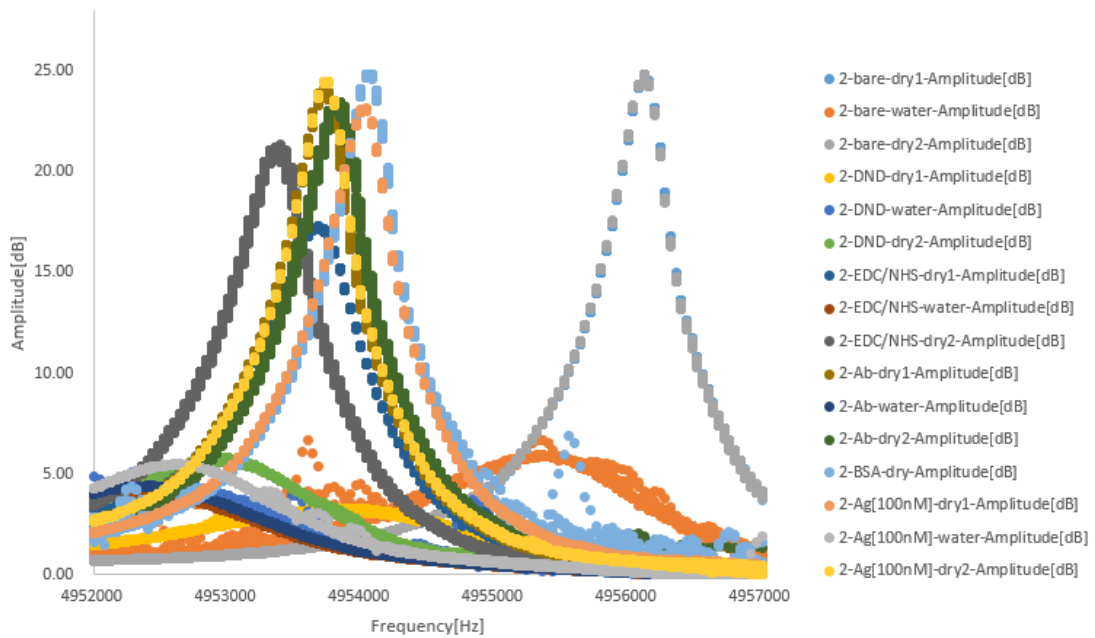


**Fig. B5.** Sensor2's amplitude.

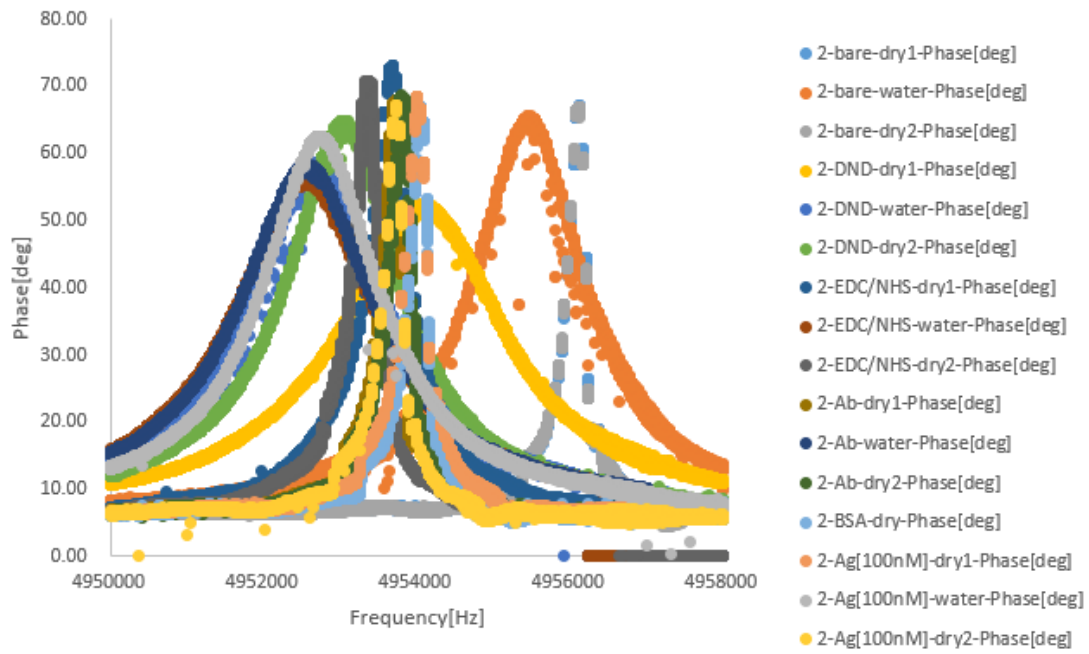


**Fig. B6.** *Sensor2's phase.*

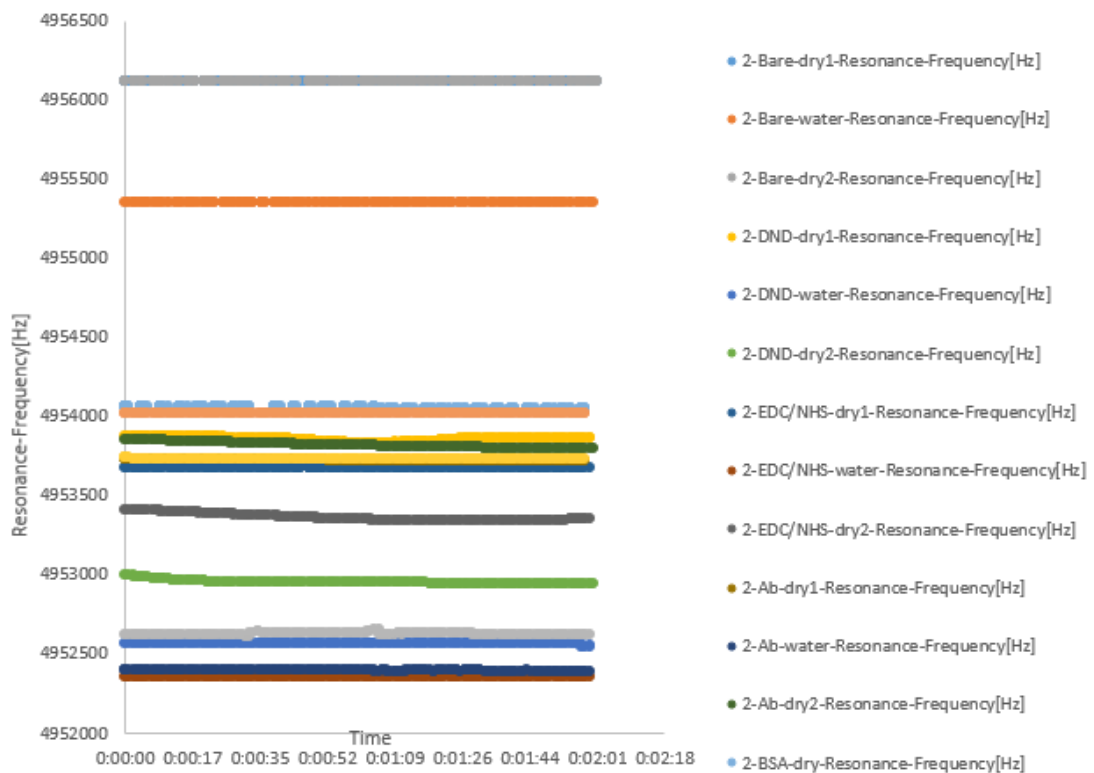


**Fig. B7.** *Sensor2's resonance frequency.*

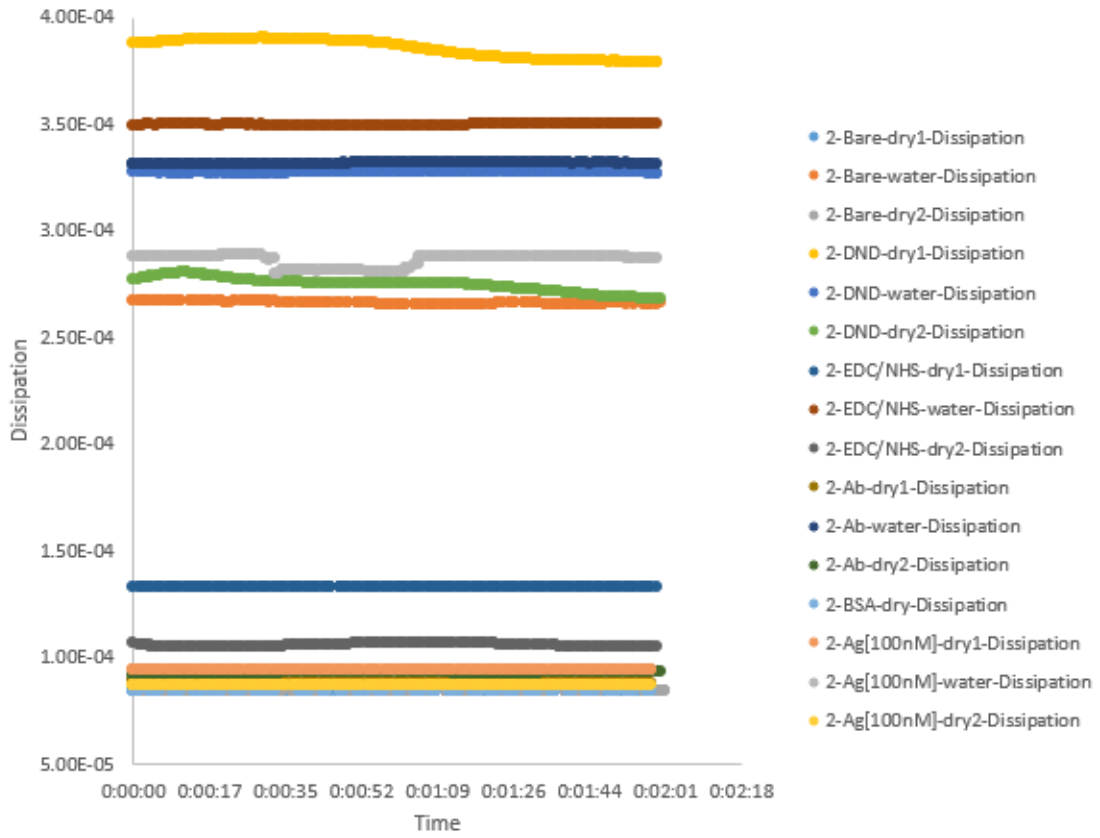


**Fig. B8.** *Sensor 2's dissipation.*

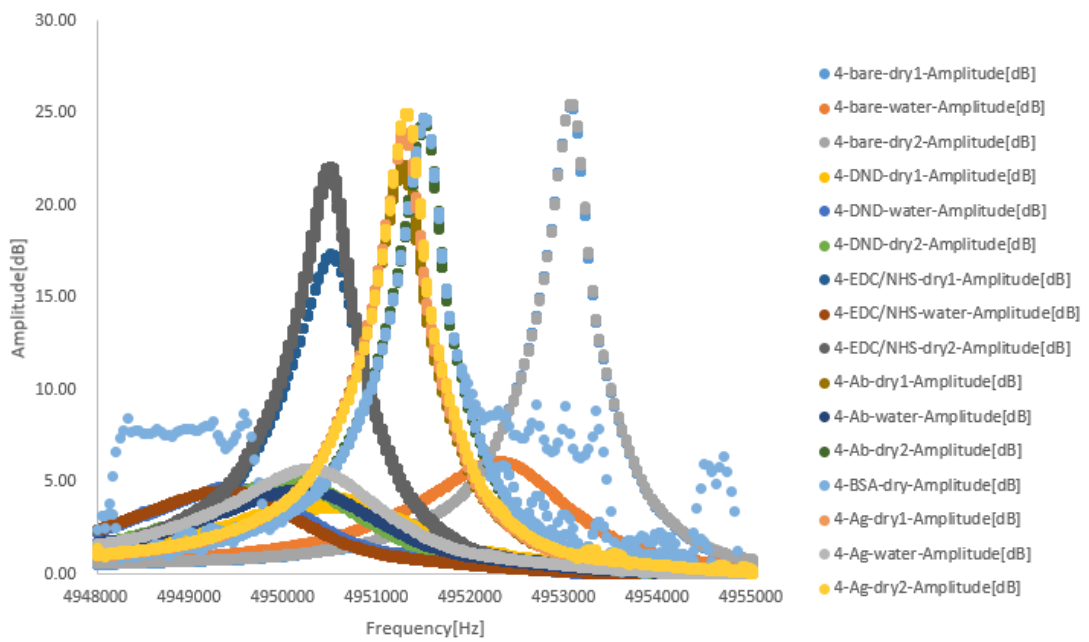


**Fig. B9.** *Sensor 4's amplitude.*

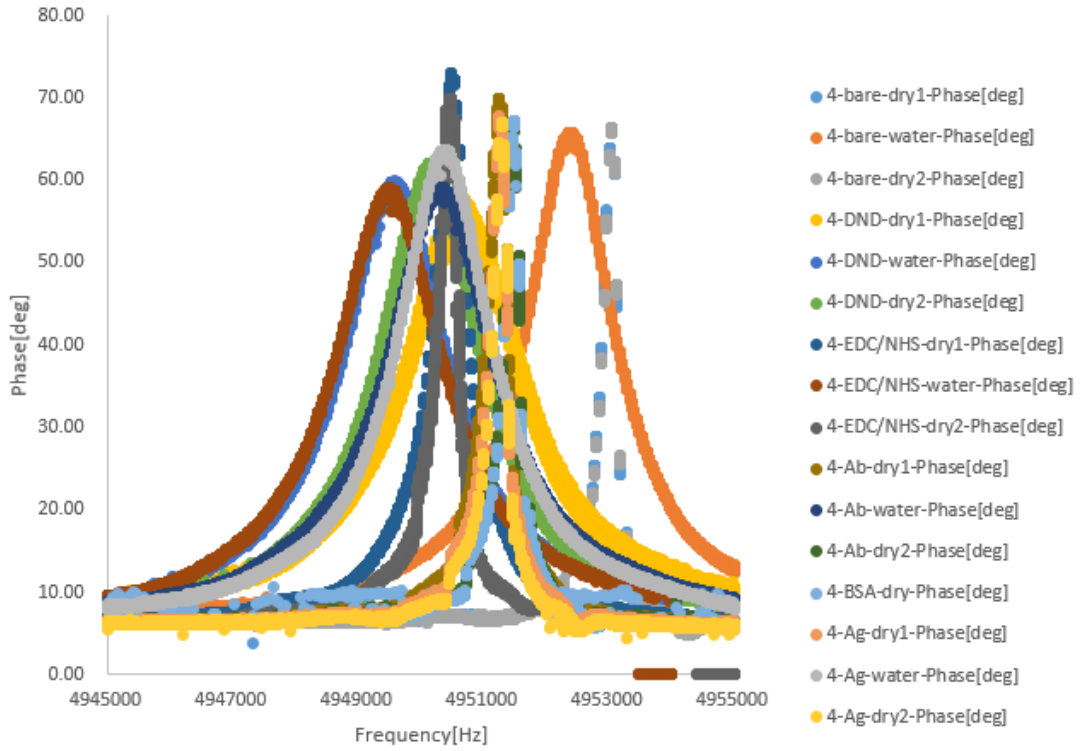


**Fig. B10.** *Sensor4's phase.*

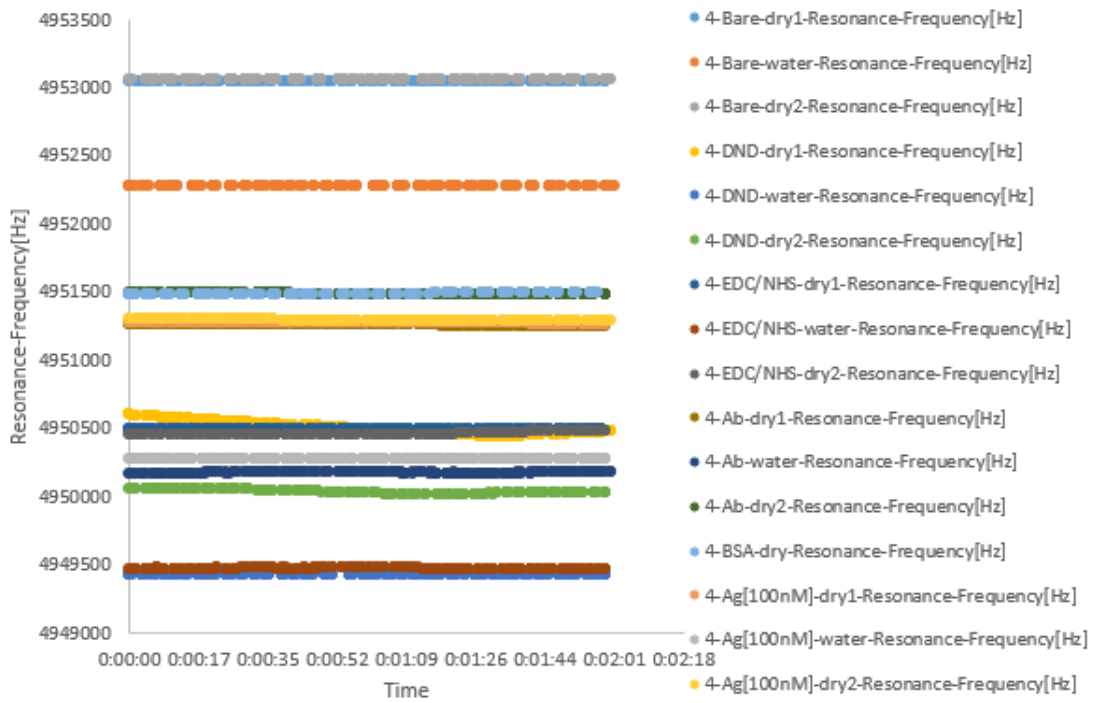


**Fig. B11.** *Sensor4's resonance frequency*

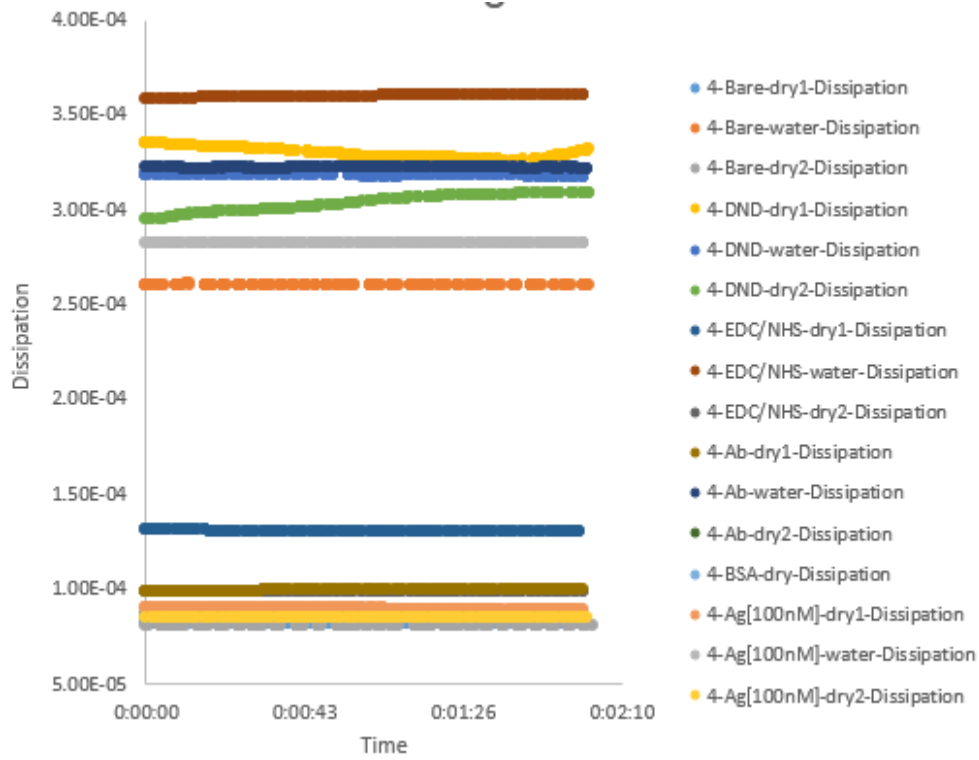


**Fig. B12.** *Sensor4's dissipation.*

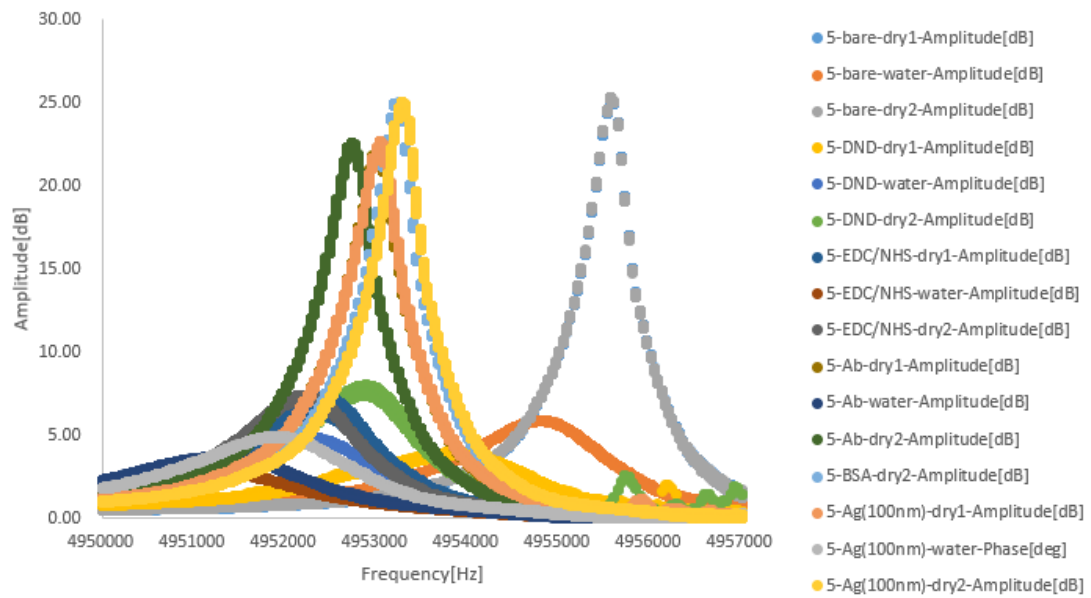


**Fig. B13.** *Sensor5's amplitude.*

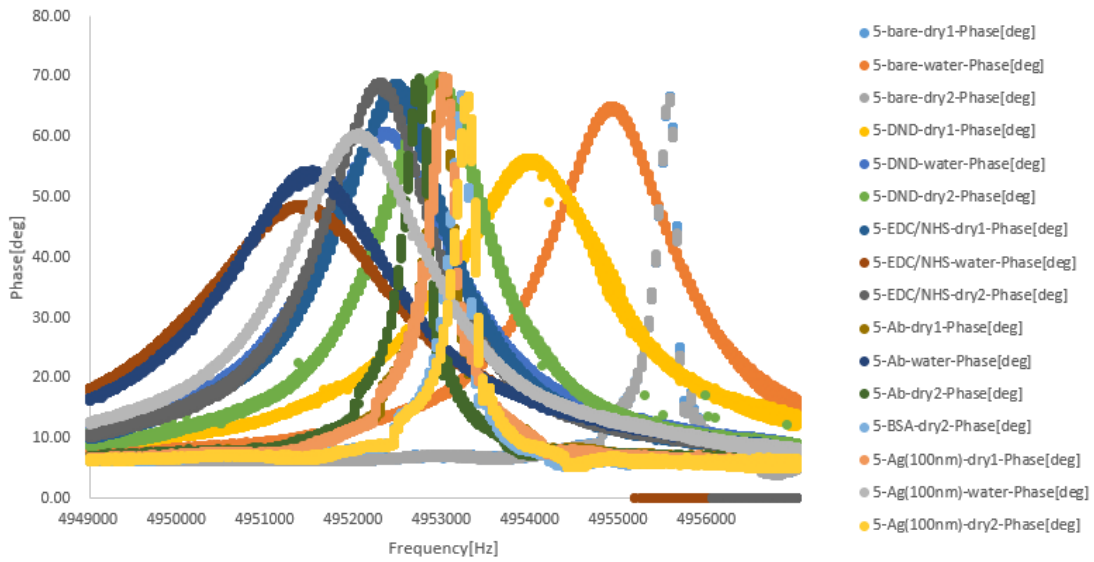


**Fig. B14.** Sensor5's phase.

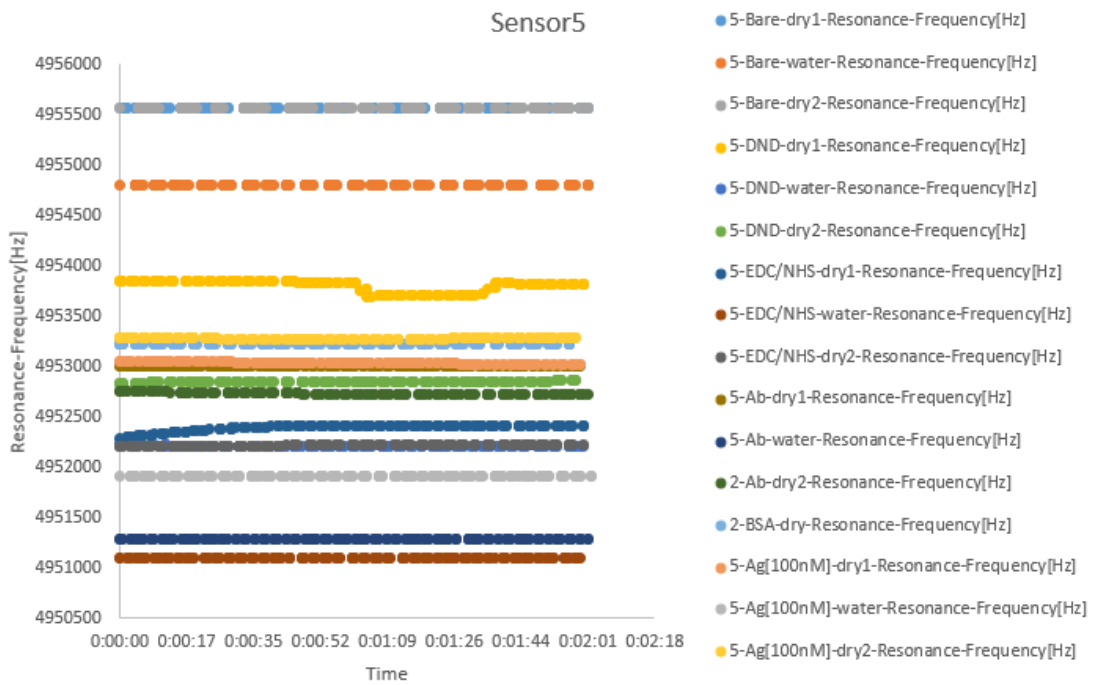


**Fig. B15.** Sensor5's resonance frequency.

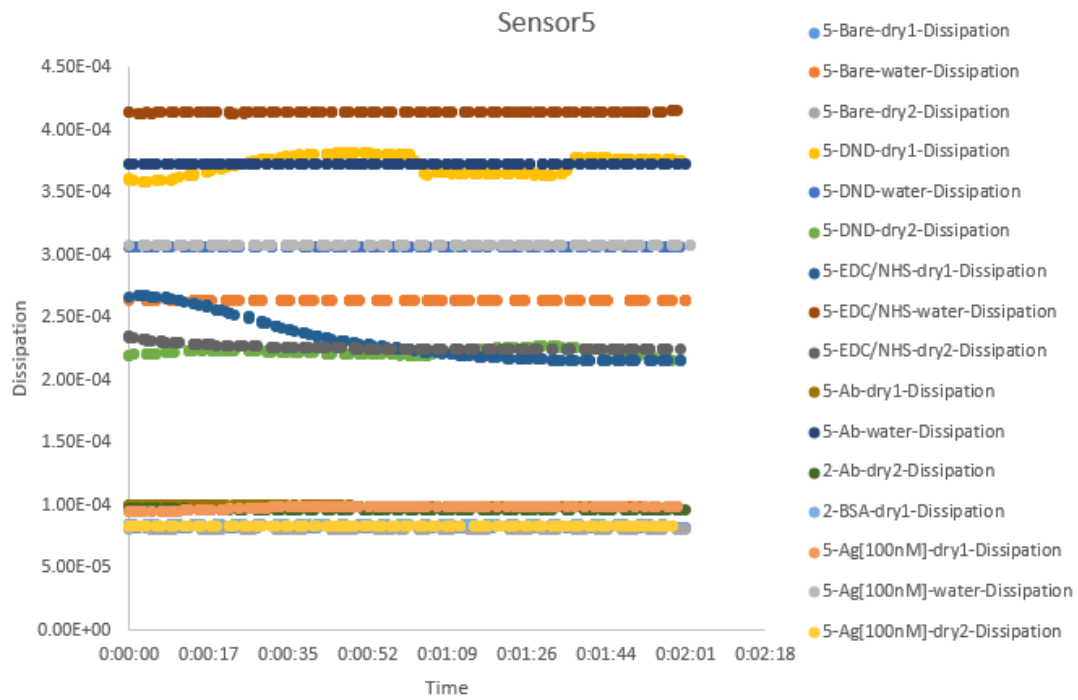


**Fig. B16.** *Sensor5's dissipation.*